Acta Geologica Sinica (English Edition), 2022, 96(1): 1–25

Special Paper for 100th Anniversary

1922—2022

Hydrodynamic Links between Shallow and Deep Mineralization Systems and Implications for Deep Mineral Exploration

CHI Guoxiang[1,*], XU Deru[2,*], XUE Chunji[3], LI Zenghua[2], Patrick LEDRU[4], DENG Teng[2], WANG Yumeng[1] and SONG Hao[5]

[1] *Department of Geology, University of Regina, 3737 Wascana Parkway, Regina, SK S4S 0A2, Canada*
[2] *State Key Laboratory of Nuclear Resources and Environment, School of Earth Sciences, East China University of Technology, Nanchang 330013 , China*
[3] *State Key Laboratory of Geological Processes and Mineral Resource, School of Earth Sciences and Resources, China University of Geosciences, Beijing 100083, China*
[4] *Université Lorraine, UMR 7359 GeoRessources, 54506 Vandœuvre les Nancy, France*
[5] *Applied Nuclear Technology in Geosciences Key Laboratory of Sichuan Province, Chengdu University of Technology, Chengdu 610059, China*

Abstract: Deep mineral exploration is increasingly important for finding new mineral resources but there are many uncertainties. Understanding the factors controlling the localization of mineralization at depth can reduce the risk in deep mineral exploration. One of the relatively poorly constrained but important factors is the hydrodynamics of mineralization. This paper reviews the principles of hydrodynamics of mineralization, especially the nature of relationships between mineralization and structures, and their applications to various types of mineralization systems in the context of hydrodynamic linkage between shallow and deep parts of the systems. Three categories of mineralization systems were examined, i.e., magmatic-hydrothermal systems, structurally controlled hydrothermal systems with uncertain fluid sources, and hydrothermal systems associated with sedimentary basins. The implications for deep mineral exploration, including potentials for new mineral resources at depth, favorable locations for mineralization, as well as uncertainties, are discussed.

Key words: hydrodynamics, structural control of mineralization, mineral systems, shallow and deep mineralization, deep mineral exploration

Citation: Chi et al., 2022. Hydrodynamic Links between Shallow and Deep Mineralization Systems and Implications for Deep Mineral Exploration. Acta Geologica Sinica (English Edition), 96(1): 1–25. DOI: 10.1111/1755-6724.14903

1 Introduction

It has become increasingly challenging to find new mineral resources at shallow depths, and mineral exploration is gradually turning to greater depths (Zhai et al., 2010; Arndt et al., 2017; Wood and Hedenquist, 2019). Accordingly, mineral exploration has become more and more risky due to increasing geological uncertainties with depth. Various mineralization models at regional to deposit scales have been developed and applied to deep exploration (Chen et al., 2006; Zhu, 2006; Wang et al., 2008; Zhai et al., 2010; Cai et al., 2015; Qin et al., 2020; Wang D H et al., 2020), commonly in combination with geophysical and geochemical methods (Huang and Xu, 2006; Song et al., 2012). While conventional mineralization models can play important roles in guiding deep mineral exploration, they also face various challenges in practical application. For example, although the zonation of alterations, mineralization styles and metal assemblages around magmatic intrusions, such as porphyry Cu-Mo deposits (Lowell and Guilbert, 1970) and granite-related Sn-W-polymetallic deposits (Jackson et al., 1989), and the relationship between porphyry and epithermal deposits (Hedenquist et al., 1998), can provide general guidance in predicting whether or not and what type of mineralization might be present at depth, the identification of specific exploration targets need additional constraints. On the other hand, although it is well known that most hydrothermal deposits are controlled by structures (Richards and Tosdal, 2001; Zhai et al., 2010; Rowland and Rhys, 2020), ore-hosting structures only represent a small portion of all the structures present in a given area, and even for the ore-hosting structures, the mineralized segments only occupy a small portion of these structures. Identifying ore-hosting structures and mineralized segments within these structures is a challenging yet critical work in deep exploration.

It is well understood that the formation of mineral deposits requires circulation of large amounts of fluids through the sites of mineralization (Chi and Xue, 2011). According to Darcy's law, fluid flow rate is related to both the permeability and driving force (hydraulic potential;

* Corresponding author. E-mail: guoxiang.chi@uregina.ca; xuderu@ecut.edu.cn

http://www.geojournals.cn/dzxbcn/ch/index.aspx; https://onlinelibrary.wiley.com/journal/17556724

Hubbert, 1940). Furthermore, it has been shown that permeability and driving force are mutually related and transient in structurally controlled fluid flow systems (Cox et al., 2001; Sibson, 2001; Cox, 2020). Therefore, the structural control of mineralization is of hydrodynamic nature. The hydrodynamic regime of mineralization systems has been the subject of numerous previous studies (Cathles, 1981; Sibson, 1987, 2001; Sibson and Scott, 1988; Cox et al., 2001; Cathles and Adams, 2005; Cox, 2005, 2020), but relatively little attention has been paid to the hydrogeological connection between the shallow and deep parts of mineralization systems in the context of deep exploration, which is the focus of this paper.

An important concept relevant to both deep exploration and hydrodynamics of mineralization is that of 'mineral systems' (Wyborn et al., 1994; McCuaig et al., 2010; McCuaig and Hronsky, 2014) or 'metallogenic systems' (Deng et al., 1999; Zhai et al., 2000, 2010; Zhai, 2007). From the view of the mineral systems concept (Wyborn et al., 1994), in which the source, path and trap constitute the essential elements of mineralization processes, hydrodynamics plays a key role in connecting the trap and the source (Hronsky, 2011). Thus, although it is not explicitly stated in the various definitions of mineral systems or metallogenic systems, hydrodynamics may be considered as an important component of these concepts. It has been proposed that one of the key elements for exploration targeting is "understanding and mapping threshold barriers to fluid flow that form extreme pressure gradients, and mapping the transient exit pathways in which orebodies form" (Hronsky, 2011; McCuaig and Hronsky, 2014), and hydrodynamics has been considered as part of shear zone mineralization systems (Deng et al., 1999). As the concept of mineral systems or metallogenic systems is increasingly employed in mineral exploration (Zhai, 2007; Zhai et al., 2010; McCuaig et al., 2010; McCuaig and Hronsky, 2014), it is important to further examine the role of hydrodynamics in ore localization (Cox et al., 2001; Sibson, 2001; Chi and Xue, 2011; Cox, 2020) in the context of deep exploration.

It should be pointed out that the meaning of "shallow" and "deep" is relative and differs depending on the time referred to (Zhai, 2007). In mineral exploration, the depth of mineral deposits generally refers to the vertical distance of orebodies from the current earth surface. Most of the mineral deposits that have been discovered so far are within 500 m from the surface (Zhai, 2007; Zhai et al., 2010; Arndt et al., 2017), and so depths <500 m may be considered shallow, and those >500 m may be considered deep. In contrast, in genetic studies of mineral deposits, the depth of mineralization refers to the depth at the time of mineralization. Because of erosion, mineral deposits that were formed at great depths may be located at shallow depths currently; conversely, in some cases, mineral deposits that were formed at shallow depths may become deeply buried at present (Zhai et al., 2010). In this paper, "shallow" and "deep" generally refer to the depth at the time of mineralization unless otherwise specified.

This paper will first summarize the principles of hydrodynamic studies of mineralization, with an emphasis on the nature of structural control of mineralization, and then provide a review of current understanding of the hydrodynamic regimes of different mineralization systems, with particular attention to the hydrodynamic link between shallow and deep parts of these systems. Finally, the significance of these studies for deep exploration will be discussed.

2 Principles of Hydrodynamic Analysis of Mineralization

2.1 Driving forces of fluid flow related to mineralization

A mineralization system generally consists of the source, path and trap of ore-forming materials (Wyborn et al., 1994). The ore-forming fluid extracted the ore-forming materials from the source, carried them through the path, and deposited them at the trap (Cox, 2005). The flow of the ore-forming fluid from the source through the path and traps plays a key role in the formation of mineral deposits. Hydrodynamic analysis of mineralization is concerned with the driving force, rate, direction and duration of the fluid flow related to mineralization (Chi and Xue, 2011).

Most hydrothermal mineralization systems may be considered as fluid flow in porous media and governed by Darcy's law, which can be expressed as:

$$q = -\frac{\rho g k}{\mu}\frac{dh}{dl} \tag{1}$$

where q is flow rate, ρ is fluid density, g is gravitational acceleration, k is rock permeability, μ is fluid dynamic viscosity, h is hydraulic head, and l is distance. Hydraulic head is related to elevation (z), fluid pressure (P_f) and fluid density as:

$$h = z + \frac{P_f}{\rho g} \tag{2}$$

which can be rearranged as:

$$\rho g h = \rho g z + P_f \tag{3}$$

The term ρgh is defined by Hubbert (1940) as hydraulic potential (Φ), i.e.:

$$\Phi = \rho g z + P_f \tag{4}$$

Using the relationships in equations (1), (2) and (4), Darcy's law can be expressed as:

$$q = -\frac{k}{\mu}\frac{d\Phi}{dl} \tag{5}$$

This equation shows that fluid flow rate is proportional to the gradient of hydraulic potential, and therefore hydraulic potential may be considered as the driving force of fluid flow. Since hydraulic potential is related to fluid pressure, elevation and fluid density as shown in equation (4), it can be deducted that the driving force of fluid flow is related to fluid pressure, elevation and fluid density.

Among the various parameters related to the fluid flow driving force, fluid pressure is of particular interest in this study because it is directly related to depth. However, it should be noted that although fluid pressure is related to hydraulic potential, fluid pressure itself is not the fluid flow driving force, and fluid does not always flow from high pressure to low pressure areas. Thus, although fluid pressure generally increases with depth, fluid does not always flow upward. This is because hydraulic potential (the driving force of fluid flow) is not only related to fluid pressure, but also to elevation and fluid density (equation 4). It can be shown that if the increase in fluid pressure with depth is governed by the hydrostatic pressure regime, i.e.,

$$P_f = \rho_f g d \tag{6}$$

where ρ_f is fluid density and d is depth (Fig. 1a), then the hydraulic potential is zero at all depths, as the elevation term (z) in equation (4) would be "$-d$" and thus

$$\Phi = \rho_f g z\,(-d) + \rho_f g d = 0 \tag{7}$$

Consequently there is no fluid flow as the hydraulic potential is zero and equal at different depths (i.e., no gradient). However, if fluid pressure is governed by the lithostatic pressure regime, i.e.,

$$P_f = \rho_r g d \tag{8}$$

where ρ_r is rock density (Fig. 1a), then the hydraulic potential will be >0 as ρ_r is $>\rho_f$:

$$\Phi = \rho_f g\,(-d) + \rho_r g d > 0 \tag{9}$$

and the hydraulic potential values will be different at different depths, which will lead to fluid flow according to equation 5. Conversely, if the fluid pressure is governed by the sub-hydrostatic pressure regime, i.e., if fluid pressure is lower than hydrostatic value:

$$P_f < \rho_f g d \tag{10}$$

then hydraulic potential will be negative, as

$$\Phi = \rho_f g\,(-d) + P_f < 0 \tag{11}$$

In such cases, the hydraulic potential will also be different at different depths, which will lead to fluid flow. In summary, if fluid pressure is governed by a hydrostatic pressure regime, the hydraulic potential will be zero and equal at different depths, and there is no fluid flow, whereas if the fluid pressure is either higher (supra-hydrostatic, e.g., lithostatic) or lower (sub-hydrostatic) than hydrostatic, the hydraulic potential will be either >0 or <0 and will be different at different depths, thus causing fluid flow.

The difference between actual fluid pressure (P_f) and the hydrostatic fluid pressure (P_h) at a given depth, $\Delta P_{f\text{–}h}$, can be expressed as:

$$\Delta P_{f\text{–}h} = P_f - P_h \tag{12}$$

If fluid pressure is higher than the hydrostatic pressure, $\Delta P_{f\text{–}h}$ is positive and is called overpressure, whereas if fluid pressure is lower than the hydrostatic pressure, $\Delta P_{f\text{–}h}$ is negative and is called underpressure (Beaumont and Fiedler, 1999; Fig. 1a). Another term that is commonly used to describe the fluid pressure regime is the pore-fluid factor (λ):

$$\lambda = \frac{P_f}{\sigma_v} = \frac{P_f}{\rho_r g d} \tag{13}$$

where P_f is fluid pressure, σ_v is vertical stress, ρ_r is average rock density, g is gravitational acceleration, and d is depth (Hubbert and Rubey, 1959). For the lithostatic regime, fluid pressure is equal to the vertical stress, and thus the λ value is 1. For the hydrostatic regime, the λ value is approximately 0.38, assuming a fluid density of 1 g/cm^3 and an average rock density of 2.65 g/cm^3.

From the above discussions it is evident that fluid pressure alone is not the driving force of fluid flow, but fluid overpressure and fluid underpressure, like hydraulic potential, can be considered the driving force of fluid flow. While fluid underpressure may be limited in time and space and may be related to special geological environments or processes, fluid overpressure is common. It is generally accepted that fluid pressure is close to the hydrostatic regime at shallow depths, and gradually changes toward the lithostatic regime with increasing depth, thus a significant portion of the upper crust is under a pressure regime between hydrostatic and lithostatic, or overpressured (Sibson, 2004), with the pore-fluid factor (λ) between ~0.4 and 1 (Figs. 1a, b). Fluid overpressure can be caused by a number of different geologic processes, which can be divided into two types, i.e., a reduction in pore space or an increase in fluid volume (Chi and Xue, 2011). In sedimentary basins, pore space reduction can result from compaction, and fluid volume increase can be caused by thermal expansion of fluid, hydrocarbon generation, and mineral dewatering, both contributing to fluid overpressure development (Bethke, 1985; Swarbrick

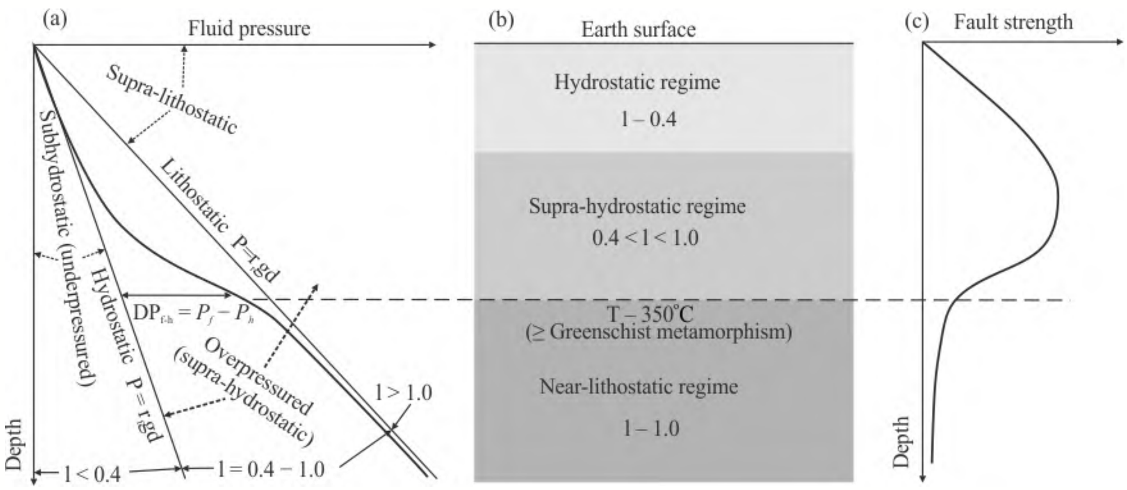

Fig. 1. (a) Depth–pressure profiles showing the various fluid pressure regimes (hydrostatic, lithostatic, sub-hydrostatic, supra-hydrostatic, and supra-lithostatic), pore-fluid factor (λ), and definition of fluid overpressure (P_f-P_h); (b) division of the upper crust into hydrostatic, supra-hydrostatic and near-lithostatic regimes; (c) profile of fault strength with depth.
(b and c are modified from Sibson, 2004).

et al., 2002). In metamorphic and deformation belts as well as in the adjacent foreland basins, fluid overpressure can be caused by compressive deformation and thrust loading as well as metamorphic dewatering (Fyfe et al., 1978; Oliver, 1986; Ge and Garven, 1992). In magmatic intrusions, the exsolution of magmatic fluids from the magmas results in an increase in the total volume, which causes fluid overpressure (Burnham, 1997). In most of the overpressured systems, fluid overpressure does not exceed the lithostatic pressure, i.e., the pore-fluid factor (λ) is generally between 0.4 and 1.0 (Fig. 1a). In some situations, however, the fluid pressure can be higher than the lithostatic value, i.e., supra-lithostatic (λ > 1.0; Fig. 1a). Such situations may be temporary and depends on the strength of the rocks, e.g., within magmatic intrusions undergoing degassing and before fracturing of the carapace (Burnham, 1997; Fournier, 1999), and in compressive, metamorphic conditions with small differential stresses (Sibson, 2004). Conversely, fluid pressure less than the hydrostatic value (sub-hydrostatic, or λ < 0.4; Fig. 1a) may be developed due to dilation of pores or abruptly opened fractures such as in a seismic event (Sibson, 1987, 2001).

When there is no fluid overpressure or underpressure, e.g., in the hydrostatic regime at shallow depths (Fig. 1b), fluid can still flow due to elevation and/or density variation, as reflected in the definition of hydraulic potential (equation 4). In such environments, fluid flow may be driven by topographic relief or take the form of fluid convection due to density variation. Topographic relief is a major driving force of modern groundwater flow systems, with water generally flowing downward in recharge areas, and upward in discharge areas (Hubbert, 1940; Freeze and Cherry, 1979). Although topographic relief is the ultimate driving force of the whole fluid flow system, elevation alone cannot determine the flow direction, as indicated by development of both downward and upward flows in the system. Therefore, the driving force is still hydraulic potential gradient, not elevation gradient. If the fluid pressure is significantly above hydrostatic regime at depth (Fig. 1a), the contribution of surface topographic relief to fluid flow will be suppressed by fluid overpressure.

Fluid convection can be driven by thermally or compositionally induced fluid density variation. Fluid density increase due to increasing total dissolved solids or salinities, such as the situation around a salt dome, can cause fluid convection (Ranganathan and Hanor, 1988). More commonly, fluid convection is related to fluid density variation due to temperature change. Fluid density decreases with increasing temperature, which can be due to increasing depths (geothermal gradient) or heat anomaly (e.g., magmatic intrusions). Vertical temperature increase with depth may or may not cause fluid convection, depending on the Rayleigh number of the system, which is determined by the geothermal gradient, rock permeability and thickness of the permeable unit (Zhao et al., 1997; Turcotte and Schubert, 2002). Although fluid convection can be developed under a supra -hydrostatic regime (Zhao et al., 1998), the hydrostatic regime is generally more favorable for development of vertical thermal gradient-induced fluid convection. Unlike the vertical thermal gradient, which may or may not cause fluid convection, however, a horizontal thermal gradient, such as that associated with a magmatic intrusion, will definitely lead to fluid convection (Norton and Cathles, 1979; Cathles, 1997). Similarly, the magmatic intrusion-induced fluid convection is better developed under a hydrostatic regime (in the country rocks) than a supra-hydrostatic regime.

In summary, at shallow depths, where the fluid pressure regime is dominantly hydrostatic (Fig. 1b), fluid flow may be mainly driven by topographic relief or fluid density variation; the former is generally unidirectional, whereas the latter commonly occurs in the form of fluid convection, which may be associated with geothermal gradient, magmatic intrusions, or local high-density brine (e.g., dissolution of salt). At greater depths, the fluid pressure regime is supra-hydrostatic (Fig. 1b), and the fluid flow is mainly driven by fluid overpressure. Fluid overpressure can also be developed at relatively shallow depths, e.g., in magmatic intrusions emplaced near surface. In all the overpressured systems, fluid flow is unidirectional, i.e., from high overpressure to low overpressure areas. The depths at which the fluid pressure transitions from hydrostatic to supra-hydrostatic depends on many factors including the permeabilities of lithological units and their spatial distribution, structures, and geothermal gradient (Sibson, 2004), which vary significantly in different geological settings (Chi and Lin, 2015). As a result, the hydrodynamic relationships between shallow and deep mineralization systems vary significantly depending on the regional and local geological environments.

2.2 Nature of structural control of mineralization

Most hydrothermal deposits, including different types formed in various geological settings, are controlled by structures (Richards and Tosdal, 2001; Vearncombe et al., 2004; Zhai et al., 2010; Chauvet, 2019a; Rowland and Rhys, 2020). Even though many studies of structural control of mineralization are mainly concerned with the geometric relationships between structures and ores as well as kinematic and stress analyses of the ore-hosting structures (Wang, 2010; Wang Z M et al., 2020; Chen et al., 2021), it is well understood that the nature of structural control of mineralization is actually about the structural control of ore-forming fluid flow (McCaffrey et al., 1999; Cox, 2005; Xu et al., 2019; Blenkinsop et al., 2020). It can be shown that the amount of ore-forming fluid flowing through a mineralization site, which determines the size and economic value of the deposit, is controlled by three factors: hydraulic potential gradient, rock permeability, and duration, all of which are related to structures. According to Darcy's law, the flow rate is proportional to the gradient of hydraulic head or hydraulic potential, and rock permeability (equations 1 and 5). Structural deformation can lead to either fluid overpressure (e.g., through compression or pore volume deduction) or fluid underpressure (e.g., through dilation associated with fracturing), both of which can create gradient of hydraulic potential and drive fluid flow (Sibson et al., 1975, 1988;

Sibson, 1987; Oliver, 1996; Cox, 2005). Structural deformation can increase or decrease rock permeability, which will enhance or impede fluid flow respectively (Caine et al., 1996; Cox et al., 2001). Furthermore, structural activity is typically episodic, and the duration of individual episodes as well as the total duration, which directly affect the amount of fluid flow through the structures, are related to the interrelationships between deformation and fluid pressure (Sibson, 1987, 2001; Sibson et al., 1988; Cox et al., 2001; Cox, 2005, 2020). Certain structural conditions have been viewed as "structural traps" catching mineralizing fluids (Chauvet, 2019a, b), however it should be cautioned that this term may be incorrectly understood as fluids being trapped and remaining stagnant. In fact, ore-forming fluids must flow through these so-called traps in order to form mineral deposits, as the metal contents in the ore-forming fluids are generally low and the amount of "trapped" fluids are insufficient to cause any significant mineralization.

2.2.1 Structural deformation as a fluid flow driving force

The role of structures in controlling fluid flow and mineralization can be divided into two categories: passive and proactive (Figs. 2a, b). For the passive role, structures merely serve as conduits (due to increased permeability) for fluid flow, whereas for the proactive role, structural activities or processes provide the driving force for fluid flow, which may be associated with seismicity (Sibson et al., 1975, 1988; Sibson, 2001; Cox, 2016). Structural processes may be divided into three stages: pre-failure, failure, and post-failure. At the pre-failure stage, the pore

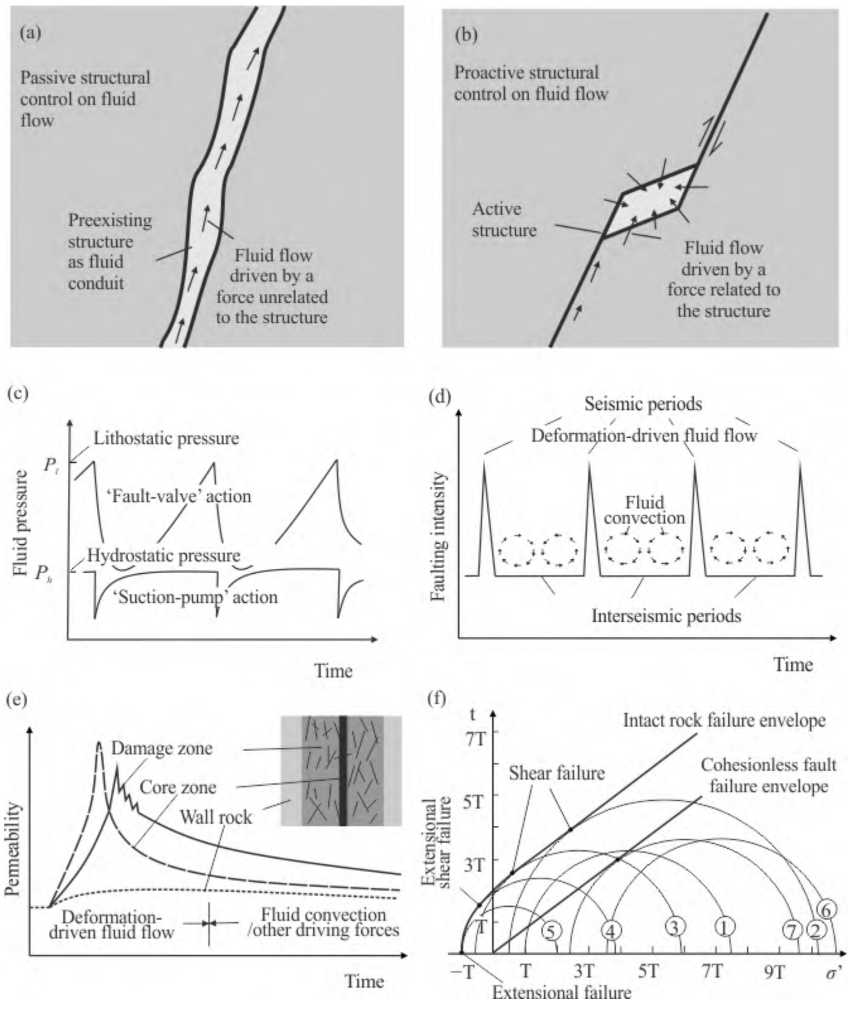

Fig. 2. (a) Passive role of structures in fluid flow–a pre-existing fault zone serving as the conduit of fluid flow; (b) proactive role of structures in fluid flow–dilation in a fault zone providing a driving force attracting fluid flow; (c) fluctuation of fluid pressure between lithostatic and hydrostatic typical of 'fault-valve' action and between hydrostatic and sub-hydrostatic typically of 'suction pump' action (modified from Sibson, 2001); (d) episodic faulting related to seismic activity alternating with interseismic periods, characterized by deformation-driven fluid flow and fluid convection, respectively (modified from Li Z et al., 2021); (e) change of permeability with time in different parts of a fault zone, showing the relatively rapid increase and decrease after faulting for the core zone, in contrast to the relatively long lasting permeability enhancement in the damage zone (based on the conceptual model of Sheldon and Micklethwaite, 2007); (f) Mohr diagrams showing how the combination of differential stress and fluid pressure control the creation or reactivation of fractures, mainly to illustrate the concept of hydraulic fracturing (see text for detailed explanations).

volume continuously changes with increasing strain, which leads to change in pore fluid pressure and creates hydraulic potential gradient, thus providing a driving force for fluid flow (Oliver et al., 2006). In a compressive stress field, increasing strain reduces pore volume (compaction) and increases pore fluid pressure, and fluid flows outward from more strained zones into less strained zones. Conversely, in an extensional stress field, increasing strain increases pore volume (stretching) and reduces pore fluid pressure, and fluid flows inward from less strained zones into more strained zones. If the initial fluid pressure regime is hydrostatic, increasing compressive strain would raise the fluid pressure toward the lithostatic regime, whereas increasing extensional strain would decrease the fluid pressure toward the sub-hydrostatic regime (Cui et al., 2012a). Generally the fluid flow rate is small at the pre-failure stage due to low permeabilities and small hydraulic potential gradients.

At the failure stage, a dramatic decrease in fluid pressure occurs within the fractured areas, regardless the stress regime. If the pre-failure pressure regime was lithostatic, the fluid pressure may drop to hydrostatic values at the failure stage, as depicted in the fault-valve model, whereas if the pre-failure pressure was hydrostatic, the fluid pressure may drop to sub-hydrostatic values, as shown in the suction-pump mechanism (Sibson et al., 1975, 1988; Fig. 2e). However, fluid pressure may also be instantly lowered to extremely low sub-hydrostatic values from pre-failure lithostatic regime, causing flash vaporization of the fluid (Weatherley and Henley, 2013). In all these cases, fluid flows toward the fractures or dilated areas, driven by hydraulic potential gradient due to pressure drop (Fig. 2b). Therefore, although compressive deformation is associated with egress flow and extensional deformation is associated with ingress flow at the pre-failure stage, ingress flow is expected at the failure stage regardless of the stress regime, as demonstrated by numerical modeling of continuous deformation of fault zones (Li et al., 2017).

At the post-failure stage, the fluid pressure regime tends to return to the original status (Fig. 2c) as a consequence of continuous ingress flow and cementation of fractures by hydrothermal minerals. Fluid flow continues to be driven by the hydraulic potential gradient between the ambience and the fractures during this period of time. If the ambient fluid pressure regime is hydrostatic, fluid flow may continue even after the fluid pressure in the fractures has resumed to the hydrostatic status, driven by topographic relief or fluid convection. The fluid convection is likely induced and sustained by the heat anomaly associated with the fluid flow driven by fluid pressure drop in the previous stage. The fluid pressure fluctuation-driven fluid flow and thermally-driven fluid convection may take place alternatingly as seismicity and associated fracturing occur episodically (Fig. 2d; Li Z et al., 2021).

2.2.2 Relationships between structures and permeability

As noted above, the relationships between structures and fluid flow may be viewed by some simply as the structures providing conduits for fluid flow due to enhanced permeabilities. The detailed relationships between structures and permeability are actually fairly complex both in space and time. It has been shown that the distribution of permeabilities along structures are typically inhomogeneous (Caine et al., 1996; Kim et al., 2004; Child et al., 2009; Choi et al., 2016), and the permeabilities evolve with structural cycles (Cox et al., 2001; Sibson, 2001; Sheldon and Micklethwaite, 2007; Cox, 2020).

Contrary to the oversimplified perception of fault zones as structures of enhanced permeabilities, they actually consist of fault core materials with permeabilities lower than the protolith and subsidiary damage zone structures with permeabilities higher than the protolith (Caine et al., 1996). The combination and distribution of these materials determines whether a fault zone will act as a conduit, barrier, or combined conduit-barrier system (Caine et al., 1996). However, the actual distribution of permeabilities in fault zones may be more complex than depicted by the core zone–damage zone model (Child et al., 2009), and the definition of 'damage zone', which include along-fault, around-tip and cross-fault varieties, may be subjective (Kim et al., 2004; Choi et al., 2016). A global compilation of structures and permeability data indicates that the fault zones in 70% of the sites investigated behave as conduits, and at least 50% of the sites contain barriers (Scibek et al., 2016). The same study also indicates that the designations of conduits, barriers or combined conduits and barriers may be biased depending on the observation method and geoscience discipline (Scibek et al., 2016). Therefore, despite extensive studies, the permeability structure of fault zones remains a complex subject which requires detailed, case by case examination. Furthermore, it should be noted that individual fault zones generally occur within a larger-scale structural network consisting of faults, fractures and shear zones that link upstream fluid reservoirs, mineralization sites and downstream outflows (Cox, 2020), and so the relationships between structures and permeability should be viewed from a regional structural perspective.

The relationships between structures and permeability should also be viewed from a dynamic perspective as permeability evolves with structural development. In particular, in low-permeability environments, high-permeability zones are generally created by fracturing, and permeability evolves as a result of dynamic competition between deformation-induced permeability enhancement and fracture- and pore-cementation processes that reduce permeability (Cox et al., 2001; Sibson, 2001; Cox, 2020). Both the permeability enhancement (fracturing) and reduction (cementation) processes related to individual structural events may be relatively short-lived (Cox, 2020), and repeated fracturing is required to account for the large amounts of fluids flowing through the fractures to form the veins and mineralization. The cyclic permeability and fluid flow evolution history likely varies at different locations of a given structure, and their time-integrated permeabilities (Sheldon and Micklethwaite, 2007) are different (Fig. 2e). It has been proposed that although the main fault in a fault zone may have high permeabilities immediately following a major slip (seismic) event, such permeabilities may be rapidly reduced due to hydrothermal cementation, whereas the damage zone may maintain high permeabilities for a longer time during the period of aftershocks (Fig. 2e; Sheldon and Micklethwaite, 2007). Thus, the damage zone has higher time-integrated permeabilities than the main fault, which may explain why secondary structures are generally more favorable for mineralization than the major faults (Sheldon and Micklethwaite, 2007).

2.2.3 Role of fluid pressure, hydraulic fracturing, and structural reactivation

The previous sections focus on the control of structures on fluid flow, either passively or proactively. However, the presence of fluids, especially their pressure regime, has important impact on structural development (Hubbert and Willis, 1957; Hubbert and Rubey, 1959; Secor, 1965; Phillips, 1972), therefore the relationships between fluids and structures are interactive (Sibson et al., 1988; Cox, 2005). Overall, high fluid pressure facilitates fracturing, which increases permeability, which in turn enhances fluid flow. On the other hand, fluid flow leads to decreased fluid pressure and permeability (due to hydrothermal sealing of fractures), which would decrease structural activities. Thus, the fluctuation of fluid pressure largely controls structural cycles, as depicted in the suction pump and fault-valve models (Sibson et al., 1975, 1988; Sibson, 2001). It should be noted, however, that the fluid pressure build up–fracturing–fluid flow cycles are not simple repetitions of the same processes and conditions, as the structures are reactivated, rather than created, in each new cycle, and the conditions for reactivation of the structures impose limitations on the maximum fluid pressure that may be sustained (Sibson, 2004; Cox, 2010).

The relationships between fluid pressure and fracturing may be described with a Mohr diagram (Fig. 2f), in which the vertical axis is shear stress and the horizontal axis is effective normal stress (Fig. 2f). The effective normal stress (σ') is expressed as:

$$\sigma' = \sigma - P_f \tag{14}$$

where σ is normal stress and P_f is fluid pressure, whereas the shear stress is unaffected by fluid pressure. The differential stress between the maximum and minimum principal stresses ($\sigma1$–$\sigma3$) is described by the diameter of the Mohr circle, the right intersection of which with the horizontal axis represents $\sigma1$ and the left intersection represents $\sigma3$. If the Mohr circle is situated within the intact rock failure envelope (circle 1 in Fig. 2f), no fractures can be produced. If the differential stress is increased, either by increasing $\sigma1$ or decreasing $\sigma3$, the Mohr circle will be in contact with the intact rock failure envelope (circle 2, Fig. 2f), and a shear fracture is produced. Alternatively, if fluid pressure is increased and so the effective normal stress is decreased, the Mohr circle is shifted leftward and touches the failure envelope (circle 3, Fig. 2f), and a shear fracture can also be produced. Fracturing commonly leads to a local decrease in differential stress (Phillips, 1972), i.e., resulting in a smaller Mohr circle than that before fracturing; a subsequent increase in fluid pressure may shift the Mohr circle leftward to touch the failure envelope in the tensile region (circle 4, Fig. 2f), resulting in an extensional shear fracture which is oblique to the least principal stress. If the local differential stress is reduced to <4T (T is the tensile strength of the rock), the subsequent increase in fluid pressure may shift the Mohr circle to touch the failure envelope on the horizontal axis (circle 5, Fig. 2f), producing an extensional fracture which is perpendicular to the least principal stress. If the effective normal stress is negative (tensile), such as circle 5 in Fig. 2f, then the extensional fracture can be called tensional fracture (Secor, 1965).

The term ‘hydraulic fracturing’, also referred to as ‘hydrofracturing’, has been extensively used in petroleum engineering, which refers to fracturing of rocks by means of fluid pressure applied in bore holes (Hubbert and Willis, 1957). According to Hubbert and Willis (1957), ‘hydraulic fractures’ refers to hydraulically induced tensional fractures perpendicular to the least principle stress. Although fractures may be produced by high fluid pressures without the need of a differential stress, which would be randomly oriented, the principle stresses are rarely equal in geological settings, and therefore hydraulic fractures generally show a preferred orientation (Hubbert and Willis, 1957). However, the term ‘hydraulic fractures’ has been used in geology in a broader sense than defined by Hubbert and Willis (1957), to include any fractures produced due to increased fluid pressure (Phillips, 1972). Thus, a hydraulic fracture can be a shear fracture (e.g., circle 3 in Fig. 2f), extensional shear fracture (circle 4, Fig. 2f), or extensional fracture (circle 5, Fig. 2f). Since a fracture may be produced by either increasing the differential stress or increasing the fluid pressure and it is generally not straightforward to distinguish the two causes, it follows that ‘hydraulic fracturing’ and ‘hydraulic fractures’ are interpretative or genetic terms rather than descriptive terms. Furthermore, since fractures may be re-opened or related to reactivated structures and fluid pressure almost always plays a role in the processes, as discussed below, such fractures may be broadly termed ‘hydraulic fractures’ too. Therefore, it is important to be aware that the meaning of ‘hydraulic fracturing’ and ‘hydraulic fractures’ may be different for different authors.

In rock bodies that have been previously fractured, the relationships between fluid pressure and fracturing or re-fracturing are more complicated than depicted by the Mohr diagram with reference to the intact rock failure envelope (Fig. 2f). Generally, the maximum fluid pressure that may be developed in such environments is lower than in intact rock bodies, and it depends on the stress regime and the strength as well as orientation of the preexisting fractures with respect to the principal stresses (Sibson, 2004; Li et al., 2019). For a given differential stress which falls within the failure envelopes of both intact rock and cohesionless fault (circle 6, Fig. 2f), a slight increase in fluid pressure would result in the Mohr circle touching the cohesionless fault failure envelope (circle 7, Fig. 2f), and so high fluid pressure cannot be reached and sustained in environments with abundant cohesionless faults. Although the cohesive strength of fractures may be restored to a value approaching that of the intact rock, the overall strength of the previously fractured rock bodies is likely lower than intact rocks, and so the maximum fluid pressure that may be restored is likely lower than the initial one within the intact rocks. It has been suggested that the fault strength increases with depth in the shallow part of the crust under the hydrostatic regime, reaches a maximum in the frictional seismogenic zone or the transitional zone between the hydrostatic and lithostatic regime, and then sharply decreases as the fluid pressure approaches lithostatic (Fig. 1c; Sibson and Scott, 1998). It has been shown that high fluid pressures may be relatively easily developed under compressional stress regime than extensional regime in fractured environments (Sibson, 2004). Under a compressional regime, supra-hydrostatic fluid pressures may be developed over a relatively wide range of differential stress, and supra-lithostatic pressure can be developed if the differential stress is sufficiently small. In contrast, under an extensional stress regime, the development of supra-hydrostatic fluid pressures requires a relatively small differential stress, and supra-lithostatic fluid pressures can be developed only if the differential stress is close to zero (Sibson, 2004).

3 Hydrodynamic Links between Shallow and Deep Parts of Mineralization Systems

The nature of the hydrodynamic link between shallow and deep parts of a mineralization system mainly depends on the driving forces of fluid flow and permeability framework, which vary with different geological environments (Chi and Lin, 2015). Hydrothermal mineralization systems may be broadly divided into those related to magmatic activities, i.e., magmatic-hydrothermal deposits, and those formed in various environments ranging from surface or near surface, sea floor, sedimentary basins to metamorphic terranes (Robb, 2020). While a generalized hydrodynamic model may be established for the magmatic-hydrothermal mineralization systems, it is impossible to build a general model for the other mineralization systems, many of which have controversial geneses. Nevertheless, these mineralization systems may be broadly divided into two groups with some commonalities in terms of hydraulic linkages, i.e., those with a strong structural control and without a close relationship with magmatism or sedimentary basins, and those within or closely related to sedimentary basins. The hydrodynamic linkages between shallow and deep parts of these different groups of mineralization systems are discussed below. It should be pointed out that these discussions are generalized, and specific mineralization systems may be variably deviated from them.

3.1 Magmatic-hydrothermal mineralization systems

The depths of magmatic-hydrothermal mineralization systems depend on the depths of emplacement of magma, which is related to the compositions of the magma. Generally, S-type granitic magmas have relatively low temperatures, high water content and low solidus, and tend to be emplaced at relatively great depths (Strong, 1988). In contrast, I-type granitic magmas typically have relatively high temperatures, low water content and high solidus, and tend to be emplaced at relatively shallow depths (Strong, 1988). Mineralization associated with magmatic intrusions may be related to the forced release of magmatic fluids due to pressure difference between the interior of the intrusions and the country rocks, and fluid convection due to the heat anomaly brought about by the intrusions, especially following the release of magmatic fluids. It can be shown that both styles of fluid flow are related to the depth of emplacement of the intrusions.

After emplacement, the magma becomes oversaturated with water either due to pressure decrease (because of movement of magma from depth to shallow levels), i.e., first boiling, or due to crystallization of anhydrous minerals, i.e., second boiling (Robb, 2020). The exsolution of magmatic fluids results in an increase of pressure within the intrusion, as the total volume of exsolved magmatic fluids plus residual magma is larger than the volume of magma before water saturation (Burnham, 1979, 1997). This effect is even more significant if we consider the scenarios of cycling of magma between the intrusion and the magma chamber as proposed by Shinohara et al. (1995), or injection of new pulses of magma and foundering of large slabs of roof rocks into the intrusion (Fournier, 1999). The pressure of the magma before water saturation is likely lithostatic as the magma is plastic and sustains the lithostatic overburden, and so the exsolution of magmatic fluids will create a supra-lithostatic pressure regime within the intrusion. However, the development and sustainability of supra-lithostatic pressure requires additional conditions, which vary depending on the depth of emplacement of the intrusions.

For deeply emplaced intrusions, the elevated ambient temperatures and relatively low permeabilities in the country rocks may help to build an effective plastic layer surrounding the intrusion, which is favorable for development of a supra-lithostatic regime. On the other hand, the relatively slow process of second boiling is unfavorable for development of a significant supra-lithostatic pressure. For shallowly emplaced intrusions, the development of supra-lithostatic pressure is generally more difficult as the fluid overpressure created by fluid exsolution may be readily dissipated by continuous fluid flow into the country rocks, which is under hydrostatic conditions. However, the relatively rapid fluid production through first boiling is favorable for fluid overpressure development. If a plastic layer surrounding the intrusion due to the heat of magma can be established to prevent slow dissipation of magmatic fluids, significant lithostatic or supra-lithostatic pressure may still be developed and maintained within the intrusion (Fournier, 1999). Such conditions can be developed as shallow as 1–2 km, and are considered to be responsible for epithermal mineralization (Fournier, 1999). The plastic layer is difficult to form by a single small intrusion, but may be created by successive emplacement of multiple intrusions, which may explain why mineralization tends to occur in the later stage of multi-phase intrusive systems (Fournier, 1999; Tosdal and Richards, 2001; Tosdal and Dilles, 2020).

The difference between the fluid pressure within the intrusion and that in the country rocks ($\Delta P_{i\text{-}c}$, where *i* stands for intrusion and *c* stands for country rock) is the main driving force of fluid flow of magmatic fluids. This pressure difference is dependent on the pressure regimes in the intrusion and the country rocks, which in turn depend on the depth of emplacement of the intrusion. At shallow depths, the fluid pressure regime in the country rocks is most likely hydrostatic, whereas the pressure within the intrusion may be lithostatic or supra-lithostatic, as discussed above. With such a contrast in fluid pressure regime between the intrusion and country rocks, the $\Delta P_{i\text{-}c}$ values increase with depth (Fig. 3a). For example, at a depth of 1 km, the hydrostatic pressure in the country rocks is approximately 100 bars, and the pressure within the intrusion is ≥270 bars (lithostatic or supra-lithostatic), thus the difference in fluid pressure between the intrusion and the country rocks is ≥170 bars. In comparison, at a depth of 5 km, the difference in fluid pressure between the intrusion (lithostatic or supra-lithostatic, ≥1350 bars) and the country rocks (hydrostatic, 500 bars) is ≥850 bars. As the fluid pressure in the country rocks gradually transitions with increasing depths into the supra-hydrostatic regime, however, the $\Delta P_{i\text{-}c}$ values will decrease with depths (Fig. 3a). As the fluid flow rate is proportional to $\Delta P_{i\text{-}c}$, and fast flowing ore-forming fluids may travel longer distance from the intrusion before precipitating ores, it may be inferred that intrusions emplaced at moderate depths (the horizontal dash line in Fig. 3a) are more likely to produce mineralization distal to the

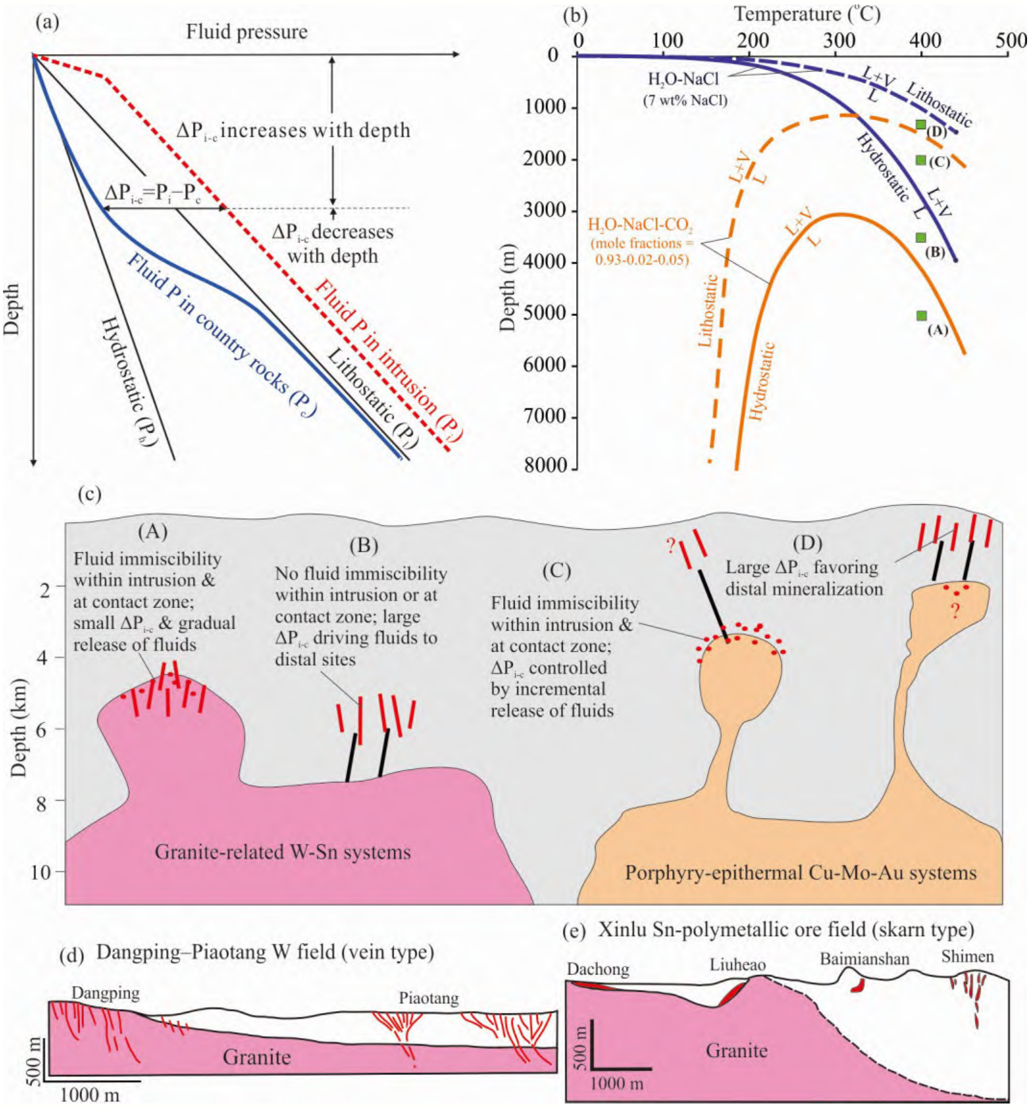

Fig. 3. (a) Depth-pressure profile illustrating the pressure difference between the magmatic intrusion (supra-lithostatic) and country rocks (hydrostatic to supra-hydrostatic) ($\Delta P_{i\text{-}c}$) and how this changes with depth; (b) phase diagrams in the depth-temperature field for H_2O-NaCl system and H_2O-NaCl-CO_2 systems showing the different depths for fluid immiscibility for hydrostatic and lithostatic pressure regimes (phase boundaries were calculated using the software of Steele-MacInnis et al., 2012, and Steele-MacInnis, 2018); (c) a schematic diagram illustrating the relatively deep emplacement for granitic intrusions and related W-Sn mineralization systems and the relatively shallow emplacement for porphyry-epithermal Cu-Mo-Au systems; note both proximal and distal mineralizations can be developed in each system, which is related to the variation of $\Delta P_{i\text{-}c}$ with depth; (d) a profile of the Dangping–Piaotang W field (modified from Tanelli, 1982) and (e) a profile of the Xinlu Sn-polymetallic ore field (modified from Chi et al., 1993), both showing proximal mineralization associated with relatively shallowly emplaced granites versus distal mineralization above relatively deeply emplaced granites. See text for detailed explanations and discussions.

intrusion, whereas intrusions emplaced at shallow or great depths tend to have mineralization proximal to the intrusion. However, there are other factors that control the localization of mineralization besides fluid flow rate, including fluid immiscibility, fluid mixing, and fluid-rock interaction. Among these factors, fluid immiscibility is closely related to fluid pressure regime and depth of emplacement of the intrusion, as discussed below.

As the release of magmatic fluids from the intrusions into the country rocks is generally accompanied by a significant pressure decrease, and fluid immiscibility is generally triggered by fluid pressure drop, the contact zone between the intrusion and the country rocks represents a potential location for fluid immiscibility and mineralization. However, it can be shown that whether or not fluid immiscibility can take place at the contact zone depends on the composition of the fluid, the pressure regime in the country rocks, and the depth of emplacement of the intrusion (Cunningham, 1978; Chi and Lu, 1991; Chi et al., 1993). For example, if the intrusion was emplaced at a depth of 5 km, and the magmatic fluid were at a temperature of 400°C when it was released from the intrusion into the country rocks (represented by point A in Fig. 3b), no fluid immiscibility would occur at the contact zone either for a fluid of the H_2O–NaCl system with a salinity of 7 wt%, typical of porphyry copper deposits (e.g., Landtwing et al., 2010), nor for a fluid of the H_2O–NaCl–CO_2 system (with 5 mole% CO_2) as is typical of granite-related Sn-W deposits (e.g., Chi et al., 1993; Yan et al., 2020). If the intrusion was emplaced at 3.5 km (point B in Fig. 3b), immiscibility would take place for the H_2O–NaCl–CO_2 fluid system at the contact zone, as the fluid pressure regime changed from lithostatic (fluid in the liquid field) to hydrostatic (fluid in the liquid + vapor field); however, for the H_2O–NaCl fluid system, fluid immiscibility would not occur because the fluid is in the liquid field for either the lithostatic or hydrostatic regime. If the intrusion was emplaced at 2 km (point C in Fig. 3b), immiscibility would take place within the intrusion for the H_2O–NaCl–CO_2 fluid system, as the fluid is located in the L + V field under the lithostatic regime; for the H_2O–NaCl fluid system, however, fluid immiscibility would not occur until the fluid was released from the intrusion (lithostatic, fluid in the liquid field) into the country rocks (hydrostatic, fluid in the liquid + vapor field). If the intrusion was emplaced at 1.3 km (point D in Fig. 3b), immiscibility would take place within the intrusion for both the H_2O–NaCl and H_2O–NaCl–CO_2 fluid systems, because at this depth both fluid systems are within the liquid + vapor field. Generally, fluid immiscibility more likely takes place for shallowly emplaced magmatic-hydrothermal systems and for those involving CO_2.

Although granite-related Sn-W mineralization systems generally formed at deeper environments than porphyry-related Cu-Mo-Au and epithermal Cu-Au-Ag systems, the distance between the mineralization and the causative intrusion vary significantly for each system, depending on the regional and local geological setting. For granite-related Sn-W mineralization systems, the orebodies may be developed within the intrusions or in the country rocks, which is related to the fluid pressure contrast between the intrusion and the country rocks as well as depth of emplacement of the granite. If the fluid pressure within the intrusion is not significantly different from that in the country rocks ($\Delta P_{i\text{-}c}$ is small), e.g., both close to lithostatic values or if the magmatic fluids were released gradually, then ore precipitation would take place within the intrusion (Fig. 3c, scenario A). Examples of such mineralization may include the W-Sn veins in the Xihuashan W deposit in south China (Tanelli, 1982; Giuliani et al., 1988; Wei et al., 2012) and those in the Cornwall district in southwestern England (Jackson et al., 1989). In addition to the possibly small $\Delta P_{i\text{-}c}$ values, fluid immiscibility may also contribute the localization of mineralization within the intrusions (Giuliani et al., 1988). However, several studies of W deposits in South China suggest that fluid inclusions in wolframite, unlike those in associated quartz characterized by the H_2O–NaCl–CO_2 system, do not show evidence of fluid immiscibility (Wei et al., 2012; Ni et al., 2015), and therefore fluid immiscibility may not be a critical factor for W mineralization within these intrusions. In contrast, if there is a significant fluid pressure difference between the intrusion and the country rocks, the ore-forming fluid may rapidly flow into the country rocks before being cooled and precipitating the ores within the intrusions, thus forming veins in the country rocks (Fig. 3c, scenario B), e.g., the Chicote Grande Sn-W deposit in Bolivia (Cox and Singer, 1996) and the Piaotang W deposit in South China (Tanelli, 1982; Ni et al., 2015). The contrasting proximal versus distal W-Sn mineralization can occur within the same ore field, e.g., the Dangping deposit within the intrusion and the Piaotang deposit in the country rocks in the Dayu W ore field (Fig. 3d; Tanelli, 1982), and the Liuheao and Dachong deposits at the contact zone (skarn-type mineralization) and the Baimianshan and Shimen deposits in the country rocks in the Xinlu Sn-polymetallic ore field (Fig. 3e; Chi et al., 1993). In both cases, the proximal deposits are associated with granites emplaced at relatively shallow depths and the distal deposits are above granites emplaced at greater depths. In the case of the Xinlu ore field, both proximal and distal mineralizations are characterized by H_2O–NaCl–CO_2 fluids that show immiscibility, and it is suggested that no proximal mineralization occurred underneath the distal mineralization because fluid flow may be too fast and fluid immiscibility did not occur at the contact zone below the distal deposits (Chi et al., 1993).

The proximal-distal mineralization patterns also apply to the porphyry-epithermal systems: the porphyry deposits which are located within the intrusions and near the contact zone (Fig. 3c, scenario C) represent proximal mineralization, and the epithermal deposits hosted in the country rocks (Fig. 3c, scenario D) represent distal mineralization. It has been proposed that high-sulfidation epithermal deposits are located above the causative intrusion, with significant input of magmatic fluids, whereas low-sulfidation epithermal deposits tend to occur a few kilometers away from the magmatic center, with the ore-forming fluids dominantly derived from meteoric water (Hedenquist and Lowenstern, 1994). According to this model, porphyry-style mineralization may be associated with the causative intrusions below the high-sulfidation epithermal deposits. However, the few examples of high-sulfidation epithermal-porphyry mineralization systems that have been reported so far are actually deviated from this model, i.e., the porphyry mineralization is not vertically below the epithermal one, but rather a few hundred meters (e.g., the Far Southeast–Lepanto porphyry-epithermal Cu-Au deposits, Philippines; Hedenquist et al., 1998) to more than one kilometer (e.g., the Zijinshan–Luoboling epithermal-porphyry Au-Cu deposits; Zhong et al., 2018) apart laterally. While preexisting structures in the country rocks may be a factor controlling the relative localization of the porphyry and epithermal deposits, the hydrodynamic regime of the intrusion and country rocks may also play a role. A $\Delta P_{i\text{-}c}$ value that is relatively small (perhaps due to slow fluid exsolution) but yet sufficient to cause effective fluid immiscibility, plus protection of a plastic layer around the intrusion (Fournier, 1999), may be favorable for porphyry mineralization and unfavorable for epithermal mineralization (Fig. 3c, scenario C). Conversely, if the $\Delta P_{i\text{-}c}$ value is so high (e.g., due to fast fluid exsolution) that the magmatic fluids burst out of the confinement of the plastic layer rapidly, then the mineralization mainly occurs at significant distances above the intrusion forming epithermal deposits (Fig. 3c, scenario D). In these scenarios, considering the total budget of ore-forming materials, the chances of finding porphyry deposits below epithermal deposits, or epithermal deposits above porphyry deposits, may not be promising. The total volume of magma and duration of magmatism, which has been considered as a more important factor than metal concentrations for the formation of porphyry Cu deposits (Chelle-Michou et al., 2017), may also be important for the potential formation and localization of epithermal deposits associated with porphyry deposits.

Based on the above discussions, the relationships between localization of mineralization and depth for magmatic-hydrothermal systems are complex and related to two main competing factors: fluid pressure contrast between the intrusion and country rocks ($\Delta P_{i\text{-}c}$), which tends to drive fluid away from the intrusion (thus favoring distal mineralization), and fluid immiscibility, which tends to localize mineralization within the intrusion or at the contact zone (i.e., favoring proximal mineralization). However, a third factor, the heat anomaly imposed by the magmatic intrusion which causes fluid convection around the intrusion (Norton and Cathles, 1979; Cathles, 1997), is also important for magmatic-hydrothermal mineralization systems. Heat anomaly is the dominant fluid flow driving force after the dissipation of the fluid pressure contrast between the intrusion and the country rocks, and is responsible for the involvement of non-magmatic fluids including meteoric fluids, through fluid convection, in the late stages of magmatic-hydrothermal mineralization (Hedenquist and Lowenstern, 1994). The duration of the heat-anomaly-driven fluid convection depends on the cooling rate of the intrusion, which is in turn dependent on the size and depth of the intrusion (Norton and Cathles, 1979; Cathles, 1997). Furthermore, as fluid convection is affected by permeability, which is strongly related to structures, preexisting structures, including those created or reactivated during the hydraulic fracturing processes related to the release of overpressured magmatic fluids in the early stage (Tosdal and Richards, 2001; Tosdal and Dilles, 2020), exert an important control on mineralization in the late stage of the magmatic-hydrothermal mineralization systems. All these hydrodynamic factors, together with geochemical factors related to different ore precipitation temperatures for different metals (metal zonation), would affect the localization of the ore deposits, which should be analyzed case by case.

3.2 Structurally-controlled hydrothermal mineralization systems of uncertain fluid sources

As introduced earlier, most hydrothermal deposits are controlled by structures. However, for magmatic-hydrothermal systems and those related to sedimentary basins, although the orebodies may be directly hosted in structures, magmatic intrusions or sedimentary basins exert the first-order control of mineralization, and therefore these deposits are not included in this section. The mineralization systems covered in this section are those that show a prominent structural control and in which the sources of fluids and metals are typically uncertain, such as orogenic-type, IOCG-type, and Carlin-type. The origins of ore-forming fluids and metals of these deposits are typically controversial and may be metamorphic, magmatic, mantle-derived, meteoric, and/or a mixture of them (Groves et al., 1998; Cline et al., 2005; Williams et al., 2005; Su et al., 2009; Goldfarb and Groves, 2015; Wang Q et al., 2021). Because of these uncertainties, the hydrodynamic linkage between shallow and deep parts of the mineralization systems is more difficult to evaluate. Nevertheless, some generalities may be envisaged, whereas specific hydrodynamic conditions and processes have to be examined case by case.

A distinct feature of the structurally controlled mineralization systems discussed here is the lack of a readily recognizable hydrogeological barrier such as the contact zone of magmatic intrusions and the basal unconformity between sedimentary basins and the basement. The upper part of the crust above the level of greenschist facies metamorphism has been described as a carapace serving as the principal load-bearing portion of the crust (Sibson, 2004), in which the fluid pressure regime ranges from hydrostatic in the upper part to supra-hydrostatic in the lower part, and below which the fluid pressure approaches lithostatic (Fig. 1b). The depth at which fluid pressure approaches lithostatic values depends on many factors including the geothermal gradient and stress regime, and has been generally considered to be 10 ± 5 km, which broadly correspond to the brittle-ductile transition zone as well as the base of the seismogenic zone, which may be up to ~20 km deep (Sibson et al., 1988; Sibson, 2004, 2019). The depths of formation of orogenic gold deposits have been generally considered to be from 3 to 15 km, and may be as deep as 20 km, however examples of gold deposits formed below 10 km are limited (Goldfarb and Groves, 2015). The mineralization environments have been divided into three zones (Groves et al., 1998), i.e., epizone (< 6 km, 150–

300°C), mesozone (6–12 km, 300–475°C), and hypozone (>12 km, >475°C) (Fig. 4a). Epithermal deposits that are controlled by structures without close association with magmatic activities may be considered as the upper part of the epizone (Rhys et al., 2020).

Most structurally controlled deposits are associated with regional-scale fault zones or shear zones, even though individual deposits are typically hosted in subsidiary structures rather than within the first-order structures. Examples of such regional structures include the Boulder–Lefroy fault in the Yilgarn craton, Australia and the Larder Lake–Cadillac fault and Porcupine fault in the Abitibi greenstone belt in Canada, for Archean orogenic gold deposits (Hagemann and Cassidy, 2000; Robert et al., 2005), and the Tan–Lu fault and Wu–Yan fault for the Mesozoic Jiaodong gold province in China (Goldfarb and Santosh, 2014; Wang Q et al., 2021). The depths of these regional faults are controversial, with opinions ranging from crustal to lithospherical or subcrustal scale, and the ore-forming fluids ranging mainly from crustal metamorphism and magmatism (Hagemann and Cassidy, 2000; Robert et al., 2005; Goldfarb and Groves, 2015) to

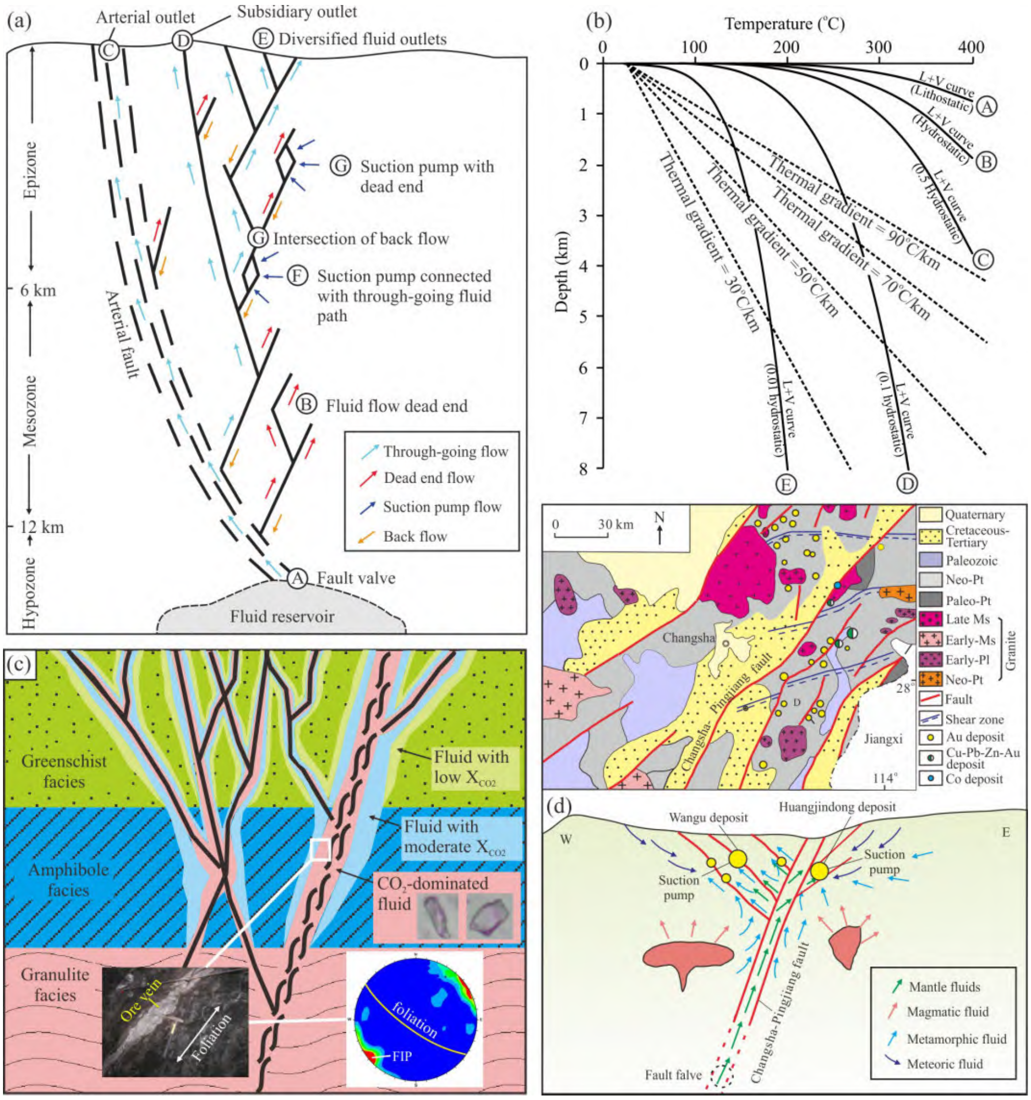

Fig. 4. (a) A schematic profile showing the relationships between a regional-scale, arterial fault and its relationships with a deep-seated fluid reservoir and lower-order faults, also showing the hypozone, mesozone and epizone as well as the concepts of suction pump, through-going flow and dead end flow, as discussed in the text; (b) a depth-temperature phase diagram for the H_2O-NaCl (20 wt%) system for various sub-hydrostatic pressure regimes showing the increasing depths of fluid immiscibility with decreasing fluid pressure and the various geothermal gradients (modified from Chi et al., 2021); (c) a schematic profile of the Red Lake greenstone belt showing the relationships between the depths of the shear zones and the composition of the ore-forming fluids, with increasing CO_2 concentrations at greater depths of the fluid sources (modified from Chi et al., 2009); (d) a simplified geological map of the NE Hunan gold district showing the distribution of gold and polymetallic deposits and their relationship with the regional Changsha–Pingjiang fault, and a schematic profile showing potential hydrodynamic relationships between the downstream, ore-controlling structures and the upstream Changsha–Pingjiang fault and its possible connection with mantle-sourced fluids as well as other potential fluid sources (meteoric, magmatic, and metamorphic), and potential fault-valve control of fluid flow at depth (modified from Deng et al., 2017). See text for detailed explanations and discussions.

the upper mantle (Goldfarb and Santosh, 2014; Wang Q et al., 2021). The concept of arterial faults, which refers to fault structures that root in portions of the crust where pore fluids are overpressured and serve as feeders for such fluids into overlying parts of the crust (Sibson, 2019), may be applied to regional faults that were developed within the crust. In the case of lithospherical fault zones tapping ore-forming fluids from the upper mantle, the second-order fault zones controlling the distribution of multiple mineral deposits may be considered as arterial faults, e.g., the Can–Cang, Jiao–Xin, and Zhao–Ping faults in the Jiaodong gold province, with mantle-derived ore-forming fluids fed by the first-order Tan–Lu fault (Goldfarb and Santosh, 2014; Wang Q et al., 2021). In this case, the first-order regional fault serves as the fluid reservoir.

The base of the arterial faults may be considered as the transitional zone between upstream fluid reservoirs and downstream fluid drainages (Fig. 4a; Cox, 2005). This is also the interval where seismic activity may be triggered through the fault valve mechanism (Fig. 4a, point A; Sibson et al., 1988; Sibson, 1990), and represent the base of the seismogenic zone (Sibson, 2019). The depths of this transitional zone are variable depending on the regional and local geological setting, and may range from 10 to 20 km (Sibson, 2019). All the mineral deposits controlled by structures, including those in the hypozone, mesozone and epizone, are located above the base of the seismogenic zone (Fig. 4a), and the study of localization of mineralization is therefore concerned with the downstream portion above the fluid reservoirs. The fault network may be divided into two types, one that is connected with the arterial fault and fluid outlets near the surface (blue arrows in Fig. 4a), and the other that has a dead end (red arrows, e.g., point B in Fig. 4a). The path of through-going fluid flow is similar to the fluid flow backbone depicted by Cox (2020), although it can be either the arterial fault with an outlet near the surface (Fig. 4a, point C) or subsidiary faults with outlets (Fig. 4a, point D). Lower-order faults with outlets (Fig. 4a, point E) can also be part of the through-going fluid flow paths, but the fluid flux is likely diminished unless they are recharged from the surface by other faults.

Dilations along some of the faults would facilitate fluid drainage from upstream, and at the same time attract fluids from surrounding rocks, functioning as suction pumps (Fig. 4a, points F and G). The fluid pressure in a suction pump cycle typically fluctuates between hydrostatic and sub-hydrostatic, in contrast to the fault valve cycle in which the pressure fluctuates between lithostatic and hydrostatic (Fig. 2c; Sibson et al., 1988; Sibson, 2001). Although the suction pump and fault valve mechanisms have been often invoked separately in different mineralizing systems, they most likely operate at the same time at different depths (Song et al., 2021), and intermediate fluid pressure fluctuations between these two endmember mechanisms are probably common in the fault network. The sudden fluid pressure drop associated with coseismic fracturing can cause fluid immiscibility, which has been considered an important mechanism of ore precipitation (Robert and Kelly, 1987; Hagemann and Cassidy, 2000; Cox, 2020; Li et al., 2020). Extreme pressure drop may cause flash vaporization and co-precipitation of quartz and gold (Weatherley and Henley, 2013). The high concentrations of CO_2, as is common in most orogenic gold deposits (Ridley and Diamond, 2000; Li et al., 2020), are favorable for fluid immiscibility to take place at great depths (Fig. 3b), especially in the mesozone (Fig. 4a). At shallower depths, especially in the upper part of the epizone, the CO_2 content is typically low and fluid immiscibility is generally difficult to happen under normal geothermal gradient and ambient fluid pressure conditions (Fig. 4b). For a H_2O–NaCl system, the fluid is located in the liquid field either under lithostatic or hydrostatic regime (Fig. 4b, curves A, B), and fluid immiscibility (boiling) will not occur unless the temperature is drastically raised by magmatic activities, such as in epithermal mineralization systems. However, if the fluid pressure is dramatically decreased below the hydrostatic level through the suction pump mechanism, fluid boiling can happen at various depths depending on the thermal gradients and the actual fluid pressure (Fig. 4b, curves C, D, E).

The dilations and suction pumps can be located along the through-going path (Fig. 4a, point F), or at a dead end (Fig. 4a, point G). Since the formation of orebodies requires large amounts of fluid passing through the sites of mineralization, the dead end sites may be unfavorable for mineralization (Cox, 2007, 2020). However, due to the fluctuation of fluid pressure in individual seismic cycles, the fluid accumulated in the dead end suction pumps, or along the dangling branches of the fault network, may back flow when fluid pressure decreases in the backbone path (Cox, 2007, 2020). The compositions of the back-flowing fluids are likely modified by fluid-rock interaction and fluid mixing along the dangling paths and suction pumps, carrying ore-forming components from the country rocks. The intersections of the backbone fault with subsidiary faults connected to the dead end suction pumps, where the back flow mixed with the through-going flow in the next seismic cycle (Fig. 4a, point H), may represent favorable site of mineralization. Although fluid pressure fluctuation has been assumed to be the main fluid flow driving force in the above discussion, it should be pointed out that fluid convection can play an important role in mineralization, especially in the inter-seismic periods, which last longer than the seismic periods (Murphy, 1979; Zhao et al., 2004; Li Z et al., 2021). The onset of fluid convection may be enhanced by the local heat anomaly brought about by the fluid flow during the seismic period, as well as the increased permeability in the fault damage zone (Cox, 2005).

From the standpoint of the relationships between shallow and deep parts of mineralization systems, it is important to realize that there is a wide range of depths at which mineralization can take place, especially in the mesozone and epizone (Fig. 4a). Many orogenic gold deposits demonstrate vertical extent of mineralization up to ~2 km or more. For example, the Au-quartz vein mineralization along the Melones fault in the Mother Lode gold belt of California extends vertically for ~1.8 km (Bierlein et al., 2008), the Jiaojia Au deposit in the Jiaodong gold province extends to a depth of ~3 km at

Zhaoxian-Wuyicun (Li Q et al., 2021), and the Sanshandao Au deposit shows economic mineralization at a current depth of 2.6 km, while thermochronological studies suggest that the upper part of the mineralization system extended above the current erosion surface (Liu et al., 2017). However, it is generally not straightforward to determine the depths of mineralization based on P–T conditions estimated from various geothermometers and geobarometers such as fluid inclusions, because there are many uncertainties regarding the fluid pressure regime (Chi et al., 2021). This is particularly true in the mesozone, where fluid pressure may range from lithostatic to hydrostatic, and even sub-hydrostatic, as discussed above. Furthermore, the potentially rapid fluid flow during seismic activity may create a very small thermal gradient within a certain depth interval, and there may be no discernable change in fluid inclusion homogenization temperatures over several kilometers depth, such as at the Sanshandao gold deposit (Hu et al., 2013).

Nevertheless, it is generally possible to assess the broad position of a given mineralization site in the hydrodynamic framework in terms of upstream versus downstream realms, and this is important for mineral exploration at depth. For example, the Red Lake gold deposit in the Red Lake greenstone belt in western Ontario, Canada consists of a number of auriferous carbonate-quartz veins hosted in metamorphosed volcanic rocks of middle greenschist to amphibolite facies (Dube et al., 2004; Chi et al., 2006a). Based on the development of banded colloform-crustiform structures of the carbonate-quartz veins and cockade breccias and the interpretation of alteration halos as pre-metamorphism, some researchers considered the mineralization to be low-sulfidation epithermal type which was overprinted by metamorphism (Penczak and Mason, 1997). However, the abundance of CO_2-rich fluid inclusions (Fig. 4c) in the veins and the estimated P–T–X conditions indicate that the mineralization is most likely of orogenic type (Chi et al., 2006a, 2009). Furthermore, the dominance of fluid inclusion planes (FIP) parallel to the foliation as well as to the auriferous quartz-carbonate veins (Fig. 4c) suggests that the differential stress ($\sigma1$–$\sigma3$) is small and the maximum principal stress ($\sigma1$) switched from horizontal to vertical during the formation of the veins (Liu et al., 2011). The small differential stress and temporally extensional stress regime indicate that the veins were formed mainly due to hydraulic fracturing related to high fluid pressures, which may be in part responsible for their apparent similarities to epithermal veins. The dominance of H_2O-free (or H_2O-invisible), CO_2-rich inclusions and the rarity of aqueous-dominated inclusions argue against the hypothesis that the CO_2-rich inclusions resulted from leakage of H_2O from original H_2O–CO_2 inclusions (Chi et al., 2006a, 2009). The greenstone belt-scale abundance of the H_2O-free, CO_2-rich inclusions is taken to support the hypothesis that the ore-controlling shear zones represent major structures that tapped the fluid reservoirs underlying the amphibolite facies host rocks (Fig. 4c; Chi et al., 2009). Therefore, the sites of mineralization in the Red Lake greenstone belt are likely located in the middle between the upstream and downstream in the fluid flow system (Fig. 4c).

In other cases of structurally controlled mineralization with uncertain origins, the sites of mineralization may be located toward the downstream of the fluid flow systems, such as many gold deposits in the Jiangnan orogenic belt in South China (Xu et al., 2017). Most of the gold deposits in the Jiangnan orogenic belt are hosted in Neoproterozoic metasedimentary rocks of lower greenschist facies, and various ages of mineralization (ranging from Neoproterozoic to late Mesozoic) and sources of ore-forming materials (ranging from metamorphic, magmatic, mantle-derived, to meteoric) have been proposed (Xu et al., 2017). Accordingly, these gold deposits have been classified as orogenic, epithermal, Carlin and magmatic-hydrothermal types by different authors (Xu et al., 2017). However, it is generally agreed that the mineralization is controlled by structures at both local and regional scales, and is developed in areas with Mesozoic tectonomagmatic activities, as exemplified by the Northeastern Hunan gold district (Fig. 4d; Xu et al., 2017; Deng et al., 2020; Zhang et al., 2020; Zhou et al., 2021).

In this district, most gold deposits are hosted in bedding-parallel fractures in the low-grade metamorphosed turbidites of the Neoproterozoic Lengjiaxi Group and are distributed in both the hanging wall and foot wall of the regional-scale Changsha–Pingjiang fault. This regional fault controlled the Cretaceous-Tertiary Changping Basin (Fig. 4d), which forms part of the late Mesozoic to early Cenozoic basin and range like tectonic province in South China due to the roll back of the Pacific plate (Xu et al., 2017). Mineralization mainly took place in early Cretaceous (Deng et al., 2017), and was controlled by reactivation of preexisting structures formed in the Early Paleozoic (Deng et al., 2020; Zhang et al., 2020; Zhou et al., 2021). Although the mineralizing fluids may be contributed by various sources including metamorphic fluids in the host rocks, magmatic fluids from nearby Cretaceous granitic intrusions, and meteoric fluids, mantle-derived fluids probably played a critical role both in terms of metal sources and hydrodynamics (Fig. 4d; Deng et al., 2017; Zhou et al., 2021). Ore-forming fluids were transported along the Changsha–Pingjiang fault and discharged into the surrounding rocks at the upper level (in the epizone), where mixing with reducing fluids enriched in Fe^{2+} attracted to suction pumps associated with fracturing in the Neoproterozoic host rocks, and reaction with Fe^{2+}-rich lithologies, resulted in sulfidation and precipitation of gold (Fig. 4d; Deng et al., 2020; Ma et al., 2021; Zhou et al., 2021). The fluid flow is likely episodic and controlled by fault valves within the Changsha-Pingjiang fault, and their activities were largely controlled by fluid pressure buildup at depth, as the transition from compressional to extensional stress regime in the late Jurassic to early Cretaceous period may be characterized by a relatively small differential stress (Zhou et al., 2021), which favors hydraulic fracturing as the main mechanism of seismicity. In this regard, it is interesting to note that the formation of porphyry and epithermal deposits has also been related to a small differential stress or a neutral stress regime (Tosdal and Richards, 2001; Tosdal and Dilles, 2020).

3.3 Sedimentary basin-related hydrothermal mineralization systems

Hydrothermal mineralization systems associated with sedimentary basins may be hosted within the basin, near the basal unconformity, and in the basement or outside the current preserved edge of the basin. Mineral deposits in each of these environments may be controlled by structures and some of them may be even related to magmatic intrusions at depth, but they are distinguished from the magmatic-hydrothermal and structurally-controlled mineral deposits discussed above in that they are related to sedimentary basins, which represent a readily recognizable reservoirs of ore-forming fluids and some ore-forming components. The hydrodynamic framework of the sedimentary basin-related mineralization systems may be divided into two first-order components: the basin and the basement, separated by the basal unconformity (Fig. 5a). The hydrodynamic regime within each component, and the relationships between them, play a major role determining the type and localization of mineralization. The basal unconformity, which is typically a paleo-weathering profile of variable thicknesses rather than a mere geometric surface, plays a critical role in the interaction between the two parts of the system (Fig. 5a). Furthermore, the geologic processes at depth, connected by deep, reactivated regional structures with the basin, may determine whether or not significant mineral deposits can form (Chi et al., 2019a, 2020).

Sedimentary basins can be formed in various tectonic settings, including foreland, intracratonic, rift, back arc, forearc, and passive margin, and fluid flow can be topography-driven, overpressure-driven, and thermally-driven (Garven and Raffensperger, 1997). The fluid flow mechanisms are strongly controlled by the fluid pressure regime, particularly hydrostatic versus supra-hydrostatic (overpressured), which are mainly controlled by the lithologies and sedimentation rate (Bethke, 1985). Fluid overpressure can result from compaction and fluid volume increase due to thermal expansion of fluid, hydrocarbon generation and mineral dewatering (Bethke, 1985; Swarbrick et al., 2002; Cathles, 2007). Abundance of fine-grained sediments (e.g., shales), which are characterized by low permeabilities, and rapid sedimentation, facilitate development of fluid overpressure, whereas coarse-grained sediments, especially sandstones that have high permeabilities, and slow sedimentation, favors hydrostatic regime (Bethke, 1985). Fluid overpressure is generally better developed in the deep and central parts of the basin than the shallow and marginal parts, and so overpressure-driven fluid flow is generally upward and toward the margin (Fig. 5a, scenario A), but downward flow is also possible if the core of fluid overpressure is located in the middle of the basin (Chi et al., 2010). In contrast, gravity- or topography-driven flow is characterized by downward movement and is generally from basin margin (topographic high) toward basin center (topographic low) (Fig. 5a, scenario B), although the fluid flow direction is upward in the discharge areas. Strongly overpressured basins, such as the Gulf of Mexico Basin, would limit the topography-driven flow to shallow-depths (Harrison and Summa, 1991), and such basins are generally unfavorable for fluid convection although it is still possible under certain conditions (Zhao et al., 2000).

The fluid pressure regime exerts an important control on localization of mineralization within sedimentary basins. Uranium deposits in sedimentary basins can be formed at various depths, from near surface to the basement, which is related to the fluid pressure regime within the basins: strongly overpressured basins favor mineralization at shallow depths, whereas nearly hydrostatic regime facilitates mineralization in the deeper parts of the basins or in the basement (Chi and Xue, 2014). This is because U mineralization is related to redox reactions, which may be controlled by the interface between the topography-driven, downward flowing, oxidizing, U-bearing fluids and the overpressure-driven, upward flowing, reducing agents-bearing fluids, and the depths of this interface depends on the relative importance of the two fluid flow driving forces (Xue et al., 2010, 2011; Chi et al., 2013; Chi and Xue, 2014). However, the role of hydrodynamics in the localization of other types of mineral deposits in sedimentary basins may not be so obvious. Most Mississippi Valley-type (MVT) Zn-Pb deposits are located at the margin of the basins, and this is related to the upward flow of basinal brines, but the driving force of the fluid flow is controversial. Some researchers believe the main driving force of fluid flow related to MVT mineralization, including the classical MVT districts in the midcontinent of the USA, is topographic relief associated with orogens adjacent to the basins (Garven et al., 1993; Garven and Raffensperger, 1997), whereas others suggest that fluid overpressure is the main driving force (Cathles and Smith, 1983; Chi and Savard, 1998; Cathles and Adams, 2005; Cathles et al., 2007). In addition to topography-driven and overpressure-driven fluid flow, fluid convection may also be an important form of fluid flow in sedimentary basins, but whether or not fluid convection actually took place in sedimentary basins without magmatic activity (Fig. 5a, scenario C) is controversial too, e.g., in the North Sea Basin (Haszeldine et al., 1984; Bjørlykke et al., 1988). Fluid convection has been proposed to have played an important role in the formation of some mineral deposits in sedimentary basins, e.g., U deposits in the Athabasca Basin (Raffensperger and Garven, 1995; Li et al., 2016), and Zn-Pb-Ag mineralization in the Mt Isa Basin (Yang et al., 2006), but these studies are generally based on numerical modeling and do not have independent evidence. However, a recent petrographic study of quartz cementation and dissolution pattern combined with reactive transport modeling provided strong evidence supporting that fluid convection indeed took place in the Athabasca Basin and played an important role in U mineralization (Wang Y et al., 2021).

The basin-basement contact has been often considered as an impermeable boundary when studying the fluid flow systems in sedimentary basins, especially in numerical modeling. However, more and more studies suggest that basinal fluids may infiltrate into the basement, either in the uppermost part (paleo-regolith; Fig. 5a, scenario D) or in significant depth of the basement (Fig. 5a, scenario E) and then recycled back into the basin (Russell, 1988; Koziy et al., 2009; Boiron et al., 2010; Richard et al., 2010; Cui et

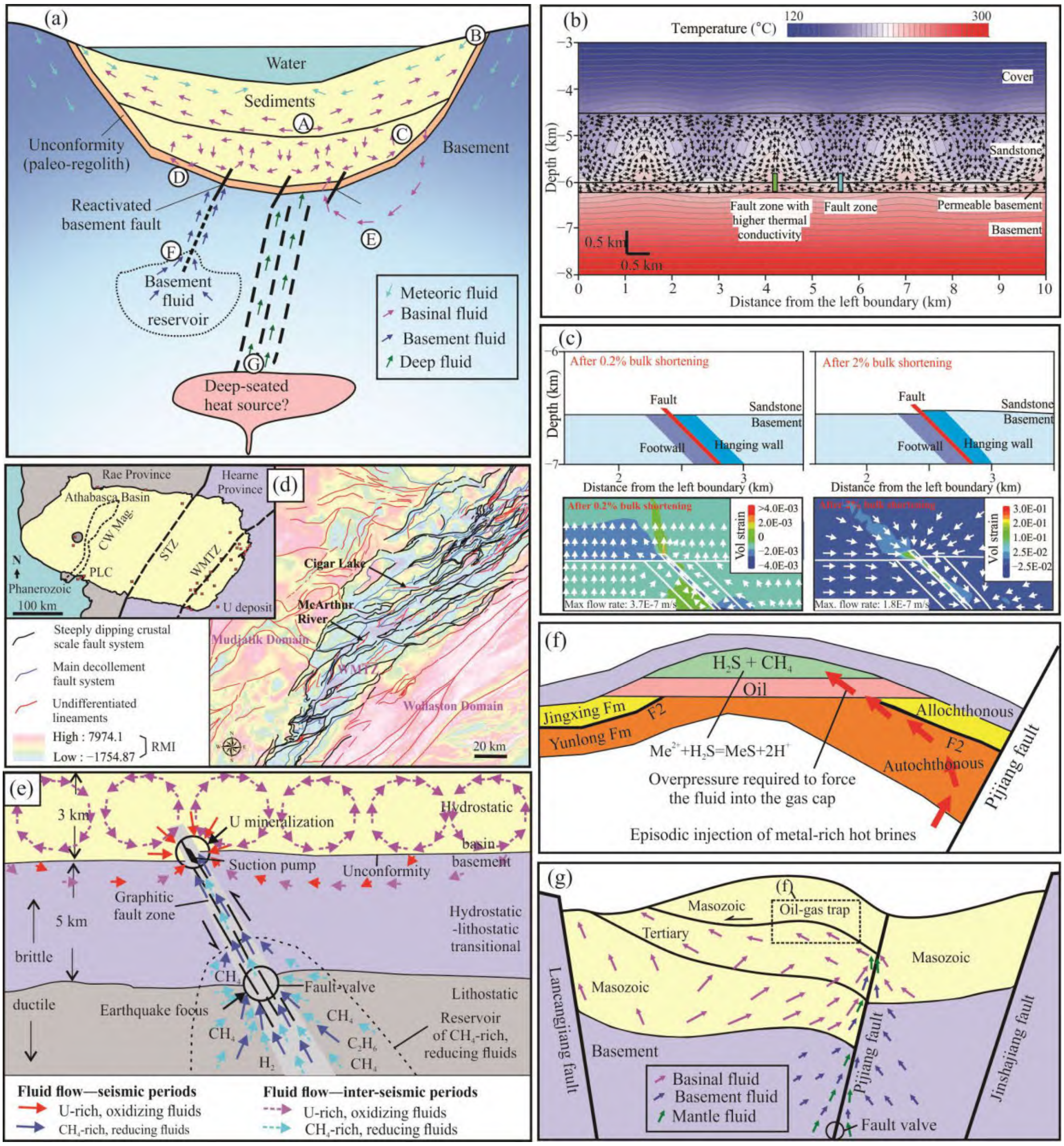

Fig. 5. (a) A schematic profile showing a sedimentary basin and its basement, separated by a paleo-regolith at the unconformity, various fluid flow patterns within the basin, reactivated basement faults connecting the basin and the basement fluid reservoirs, and regional deformation zones connecting with deep-seated heat and fluid sources; (b) numerical model of fluid convection showing egress flow along a basement fault with a relatively high thermal conductivity and ingress flow along an adjacent basement fault (modified from Li et al., 2016); (c) numerical modeling of fluid flow driven by compressive deformation showing egress and ingress flow at relatively low and high degree of deformation, respectively (modified from Li et al., 2017); (d) a simplified geological map of the Athabasca Basin showing the distribution of unconformity-related U deposits and their relationships with regional structures (modified from Card, 2020) and a map showing residual magnetic intensity and linear structures in the Wollaston–Mudjatik transition zone (modified from Ledru et al., 2022); (e) a schematic model showing fluid flow related to faulting along a graphitic basement fault in the Athabasca Basin, with a fault-valve action at depth and a suction pump action at the upper tip of the fault near the unconformity, as well as fluid convection dominating in the periods between episodic faulting (modified from Song et al., 2021); (f) a schematic model showing the formation of the Jinding Zn-Pb deposit by forceful injection of hot metal-bearing brines into the gas cap of a paleo-oil-gas reservoir (modified from Chi et al., 2017); (g) a schematic profile of the Lanping Basin showing potential role of the regional-scale Pijiang fault in the formation of the Jinding deposit, emphasizing the contribution of extra-basinal fluids in building an overpressured ore-forming fluid system (modified from Xue et al., 2006).

al., 2012b; Mercadier et al., 2012; Bons et al., 2014; Li et al., 2016, 2017, 2018; Pek and Malkovsky, 2016; Rabiei et al., 2021). The ingress (from basin into basement) and egress (from basement into basin) fluid flow may be driven by fluid density variation or deformation (Figs. 5b, c). Fluid convection due to fluid density variation may be caused by salinity change (Koziy et al., 2009; Bons et al., 2014) and geothermal gradient (Li et al., 2016; Pek and Malkovsky, 2016). Ingress flow may occur along some reactivated basement faults and egress flow occurs along other faults, depending on the location, spacing and thermal properties of the faults (Fig. 5b). Reactivated basement faults extended into the basin have been shown to be promoting egress fluid flow (Eldursi et al., 2021). Deformation-driven fluid flow is strongly dependent on the stress field, with ingress flow being generally related to extensional stress regime and egress flow to compressional one (Oliver et al., 2006; Cui et al., 2012a). However, it has been shown that both ingress and egress flow can be developed in a compressional stress regime, depending on the degree of deformation (Fig. 5c; Li et al., 2017), and both of them may occur simultaneously at different localities under the same stress field, depending on the mechanical properties of the rocks (Li et al., 2018). Furthermore, it has been shown that fluid convection may be impeded by deformation (Oliver et al., 2006; Li Z et al., 2021) and fluid convection and deformation-driven flow may occur alternatingly (Li Z et al., 2021).

The basement of sedimentary basins generally experienced multiple tectonic deformation events and contains numerous pre-existing faults. As discussed above, the reactivation of these faults plays a major role in inducing basinal fluid into the basement. Similarly, these faults also play a major role in driving basement fluids into the basin (Fig. 5a, scenario F; Fayek and Kyser, 1997; Li et al., 2017, 2019; Song et al., 2021). However, it is known that only a small number of the basement faults are related to mineralization, and even in these faults, only a small portion is mineralized. This raises the question about what kind of basement structures are more likely to be reactivated and connected with the fluid reservoirs in the basin and in the basement. Furthermore, it is known that not all sedimentary basins are equally endowed with mineral resources, and even in a given sedimentary basin, mineral deposits are commonly concentrated along certain basement structures, which raises the question about whether or not, and how, regional-scale, deep-seated structures play a role in mineralization (Fig. 5a, scenario G). These questions are generally difficult to answer, and should be evaluated case by case. However, there are more and more examples indicating that the coupling between intra-basinal and deep-seated geologic processes plays a critical role in the formation of major deposits in sedimentary basins (Chi et al., 2019a). Three such examples, including U deposits associated with granitic and volcanic rocks in South China and the Beaverlodge U district in Canada, the unconformity-related U deposits in the Athabasca Basin in Canada, and the Jinding Zn-Pb deposit in the Lanping Basin, southwestern China, are discussed below.

Granite-related and volcanic-related U deposits in South China are among the most important types of uranium deposits in China (Xu et al., 2021). Although these deposits are structurally controlled and are not directly hosted in sedimentary basins or at the unconformity, most of them are spatially and temporally close to the Cretaceous and Tertiary red bed basins, and they are interpreted to be related to fluids derived from these basins (Chi et al., 2020; Guo et al., 2020). Similarly, the U deposits hosted in metamorphic granitic rocks and amphibolite in the Beaverlodge district in Canada are spatially and temporally associated with the Paleoproterozoic Martin Basin, and the mineralization is interpreted to be related to the basinal fluids (Liang et al., 2017; Chi et al., 2020). In both cases, the U mineralization took place in a period when the tectonic setting changed from compressive to extensional regime, accompanied by mantle-derived magmatism, and it is therefore proposed that the mineralization was controlled by both basinal and deep-seated geological processes (Chi et al., 2020; Guo et al., 2020).

The Paleo- to Mesoproterozoic Athabasca Basin hosts a number of world-class U deposits with the highest grades in the world (Jefferson et al., 2007; Kyser and Cuney, 2015). These deposits are mostly located near the unconformity between the basin and the underlying Archean and Paleoproterozoic metamorphic rocks, and are named unconformity-related uranium (URU) deposits (Jefferson et al., 2007; Kyser and Cuney, 2015). However, some of the orebodies may extend to ~1 km below the unconformity (Potter et al., 2020; Rabiei et al., 2021). All the deposits are controlled by reactivated basement faults crosscutting and reversely offsetting the unconformity surface, and many of these faults are developed within graphitic lithologies (Jefferson et al., 2007; Kyser and Cuney, 2015; Potter et al., 2020). The URU deposits have been broadly classified into two types, one that is mainly developed above the unconformity, polymetallic (containing Ni-Co-Cu-As in addition to U) and has a broad alteration halo suggesting an egress fluid flow, and the other that is developed within the basement, monometallic (U) and has a narrow alteration halo indicating an ingress fluid flow (Jefferson et al., 2007). Most of the URU deposits in the Athabasca Basin are distributed along regional scale deformation zones, especially the Wollaston-Mudjatik transition zone (WMTZ), the Snowbird tectonic zone (STZ), and the Patterson Lake corridor (PLC) near the Clearwater magnetic domain, which is within the regional Fond du Lac gravity low (Fig. 5d; Card, 2020).

The ore-forming fluids are mainly basinal brines derived from sea water evaporation (Richard et al., 2011; Mercadier et al., 2012), and the sources of the U have been controversial, including a basement origin (Richard et al., 2010) and basinal origin (Chi et al., 2019b). The depth of mineralization was conventionally considered to be >5 km, but based on regional geochrono-stratigraphic data, it has been proposed that the deposits were formed at depths of <3 km (Chi et al., 2018). This difference in mineralization depth estimation has important implications on the hydrodynamic regime and the geothermal gradient, both affecting the potential mechanisms of fluid flow related to U mineralization. A shallow burial environment, together with the sandstone-dominated nature of the basin sediments, favors a hydrostatic regime in the basin (Chi et al., 2013), instead of a lithostatic regime as assumed in the conventional model. A hydrostatic regime facilitates establishment of fluid convection in the basin, which is further enhanced by elevated geothermal gradients as implied by high temperatures at shallow depths (Wang Y et al., 2021). Furthermore, a hydrostatic regime at the base of the basin in a shallow burial environment suggests that the unconformity surface is unlikely a hydraulic interface between hydrostatic and lithostatic regime; such an interface is likely located at greater depths in the basement (Fig. 5e). This hypothesis is supported by the study of graphite in basement faults hosting URU deposits (Song et al., 2021), which suggests that the faults may be reactivated due to the fault-valve mechanism ~5 km below the unconformity surface, whereas the upper tip of the faults may attracts fluids both from the basement and basin via the suction pump mechanism (Fig. 5e). Thus, the formation of the URU deposits may be considered a result of coupled fault-valve and suction pump mechanism. Furthermore, fluid convection during the periods between individual faulting events may further contribute to the mineralization (Fig. 5e). The regional strain field (Fig. 5d), characterized by steeply dipping anastomosing fault systems that extend over several hundred kilometres along strike, is interpreted as resulting from the horizontal shortening and vertical stretching of a weak lithosphere during Paleoproterozoic orogens (Gapais, 2018; Poh et al., 2020; Ledru et al., 2022). In this model, deeply rooted structures like the Wollaston–Mudjatik Transition Zone, the Snowbird Tectonic Zone/Virgin River shear zone and the Patterson Lake corridor, are responsible of crustal segmentation and are natural links between deep and shallow processes. Their evolution during the late orogenic stages also contributes to the segmentation of the crust as they guided in many cases the intrusion of magmatic bodies extracted from the mantle or generated during crustal melting and have recorded significant retro-metamorphic evolution and hydrothermal alteration. Moreover, they have been preferably reactivated after the deposition of the Athabasca basin due to increased fluid pressure and geothermal gradients imposed by the deep processes. Thus, they are considered as having played a critical role in connecting the sites of mineralization near the unconformity with deep-seated heat source and reducing agents (Chi et al., 2018; Ledru, 2019; Potter et al., 2020). The coupling of these deep-seated processes with the development of uraniferous brines within the basin is the critical factor for the rich endowment of U deposits in the Athabasca Basin (Chi et al., 2019a, b).

The Jinding Zn-Pb deposit, located in the Meso-Cenozoic Lanping Basin in southwestern China, is the largest sandstone-hosted Zn-Pb deposit in the world and has been the subject of numerous studies, including those related to hydrodynamics of mineralization (Kyle and Li, 2002; Xue et al., 2003, 2006, 2007, 2015; Chi et al., 2006b, 2007, 2012, 2017; Leach et al., 2017; Song et al., 2020; Mu et al., 2021). The deposit is hosted in a structural dome consisting of Mesozoic sandstone and limestone thrusted over Tertiary sandstone that is located near the reginal Pijiang fault (Figs. 5f, g) (Third Geological Team, 1984). It is generally believed that the deposit formed from reaction between metal-rich brines and H_2S derived from bacterial sulfate reduction associated with a paleo-oil-gas reservoir hosted in the Jinding dome (Xue et al., 2015; Chi et al., 2017; Mu et al., 2021). However, there are significant disagreements regarding the nature of mineralization (Kyle and Li, 2002; Xue et al., 2003, 2007; Leach et al., 2017; Song et al., 2020; Mu et al., 2021). Some researchers suggested that mantle-derived fluids made significant contributions to the metal budget based on Pb and noble gas isotopes (Xue et al., 2003, 2007), whereas other researchers emphasized the similarities of the mineralization characteristics with MVT deposits (Leach et al., 2017; Song et al., 2020) and sediments in the basin as the major source of metals, although some contribution from the basement is not excluded (Mu et al., 2021).

From the point of view of hydrodynamics of mineralization, it is important to examine the controlling factors of fluid flow related to mineralization. Fluid inclusion data and sand injection structures suggest that the mineralizing fluids were significantly overpressured (Chi et al., 2007, 2012), which is also required for the metal-carrying fluids to reach the H_2S in the gas cap in order to precipitate the metals in the paleo-oil-gas reservoir (Fig. 5f). Numerical modeling suggests that significant fluid overpressure could not be generated by sediment compaction alone, and input of extra-basinal fluids, such as from the mantle, is required to explain the fluid overpressure (Chi et al., 2006b). The widespread development of breccias in the deposit has been related to hydraulic fracturing due to fluid overpressure (Chi et al., 2007, 2012), however it has been alternatively interpreted as a result of evaporite diapirism (Leach et al., 2017; Song et al., 2020). Although both interpretations agree on the presence of fluid overpressure, they have different implications on what controlled the mineralization: intra-basinal versus extra-basinal. The evaporite diapirism is mainly an intra-basinal process, whereas fluid overpressure due to external fluid input is related to extra-basinal processes, such as mantle degassing. While it is possible that metals were mainly derived from the basin and evaporite diapirism is mainly responsible for the formation of the breccias, we are more inclined to believe that the hydrodynamic system controlling the mineralization of the Jinding deposit is related to deep-seated processes. It has been postulated that overpressures may be related to direct linkage between regional faults and mantle degassing (Sibson, 2001), such as the San Andreas fault system (Kennedy et al., 1997). Such deep-seated processes regulated the fault-valve mechanism along the Pijiang fault at depth (Fig. 5g), resulting in episodic faulting and pulses of forced fluid flow.

4 Discussion and Implications for Deep Mineral Exploration

The reviews of the principles of hydrodynamics of mineralization and their applications in various mineralization systems above indicate that while we have some general understanding about the factors controlling the fluid flow related to mineralization, including driving forces and distribution of permeabilities, there are many uncertainties about the detailed flow paths and their connectivity. Thus, although there have been continuing efforts in applying modeling of fluid flow to mineral exploration (e.g., Hobbs et al., 2000; Liu et al., 2010; Zhang et al., 2011; Chi et al., 2019c), significance of such studies remains more qualitative than what might be implied by the name 'numerical modeling'. Nevertheless, the principles and case studies reviewed in this paper provide valuable insights on deep mineral exploration, including potentials for new mineral resources at depth, favorable locations for mineralization, and uncertainties, which are further discussed below.

A question that exploration geologists keep asking themselves is: what is the potential to find new mineral resources at depth? From the point of view of hydrodynamics of mineralization, in addition to knowing the type(s) of mineral deposits sought after, it is important to evaluate the vertical extension of the hydrological framework and the position of the currently shallowly buried areas in the paleo-hydrological system related to mineralization, i.e., upstream versus downstream. If it is located downstream, the possibility of finding mineralization at depth is relatively high, although the types or styles of mineralization may be different. Conversely, if it is located upstream in the paleo-hydrological system, such as the hypozone (Fig. 4a), then the chance of finding significant mineralization at depth would be slim. However, being located downstream does not necessarily mean there is mineralization at depth, as there are multiple factors that control whether mineralization took place at depths, including fluid pressure, temperature, fluid immiscibility, fluid mixing, and fluid-rock interactions. For example, in the Xinlu Sn-polymetallic ore field, it is predicted that in locations where distal mineralization is well developed, proximal mineralization at depth is unfavorable (Fig. 3e; Chi et al., 1993). Another example is the sandstone-hosted U mineralization in the Ordos Basin: although the discovered deposits are located at relatively shallow depths and might be considered as the downstream of upwelling basinal fluids, the probability of finding significant U mineralization at great depths, e.g., near the basal unconformity, is considered low because the fluid overpressure at depth is unfavorable for U-bearing fluids to infiltrate (Xue et al., 2010, 2011; Chi and Xue, 2014). In contrast, in the Northeastern Hunan Au district in the Jiangnan Orogen, the currently discovered Au deposits are considered to be located downstream in the paleo-hydrogeological framework (Fig. 4d; Deng et al., 2017, 2020; Zhou et al., 2021), and therefore the probability of finding significant Au mineralization at depth is considered high. In particular, since this area is located in the epizone, the top 2 km depths may still contain significant amounts of undiscovered epizonal and mesozonal Au deposits as long as other favorable mineralization conditions (e.g., chemical traps in the Neoproterozoic metasedimentary rocks) extend to such depths. In the Athabasca Basin, the unconformity-related uranium deposits may occur in the sandstone immediately above the unconformity (egress style mineralization) or deep (up to 1 km) in the basement (ingress style mineralization). A question that may be considered in exploration is: in a structure that contains egress style mineralization, is there the possibility of finding ingress style mineralization at depth? According to the numerical modeling of fluid flow related to compressive deformation (Li et al., 2017), both ingress flow and egress flow may occur in the same fault during the deformation history, and therefore the possibility of finding basement-hosted orebodies below sandstone-hosted ones cannot be discounted.

It is well known that structures that host mineral deposits only represent a small portion of the numerous structures present in any crustal environments. A question that follows is how we know what structures are more likely to host mineral deposits. While there is not straightforward answer to this question, empirical observations indicate that lower-order structures close to regional-scale structures are generally more favorable than those far away from the regional structures. This appears to be true not only for structurally controlled mineralization with uncertain fluid origins, but also for magmatic-hydrothermal deposits and those related to sedimentary basins. From the point of view of hydrodynamics of mineralization, this is likely related to the hydrological connectivity of subsidiary structures with the regional structures, which may have played two critical roles: connection with the sources (reservoirs) of the ore-forming fluids, and facilitating the episodic reactivation of the subsidiary structures to pump fluids from the arterial or backbone flow path. For magmatic-hydrothermal deposits, although the intrusions may seem to be the first-order control of mineralization, the intrusions themselves, together with the magma chamber, are actually controlled by regional-scale structures, which may also serve as the conduits for fluids derived from magma chambers to be channeled to the sites of mineralization (Tosdal and Richards, 2001; Tosdal and Dilles, 2020). In the Athabasca Basin, the reason why the U deposits are concentrated along some regional structures (Fig. 5d) has not been well understood, as the basement rocks in these structures do not show any particular U fertilities and it has been demonstrated that U may have been mainly derived from the basin (Chi et al., 2019b). The most likely role of the regional structures is that they facilitated the reactivation of the basement faults near the unconformity, which enhanced the permeability, provided the driving force of fluid flow, and promoted exchange of fluids between the basin and the basement (Fig. 5e). For the Jinding Zn-Pb deposit, although it may look like a mineralization similar to MVT deposits, the regional Pijiang fault probably played a critical role in providing deeply sourced fluids and driving the forceful fluid flow. This has important implications for guiding regional exploration: if the mineralization is considered as related to intra-basinal processes, including evaporite diapirism, then geological factors controlling mineralization would be sought within the basin. Conversely, if the regional structures played a major role, the areas adjacent to these structures should be considered more favorable than other areas.

Even if we can identify structures that are more likely to host mineral deposits, we still face yet another question: since most ore-hosting structures are linear and the mineralized segments represent only a small port of them, what control the localization of orebodies within these structures? Empirical observations have shown that intersections of faults and segments with change in fault orientation are favorable for mineralization, and this is generally attributed to enhanced permeabilities facilitating fluid flow. However, there are more exceptions than actual mineralization for such structural sites. One possibility is that many of such sites of enhanced permeabilities are not connected with the arterial or backbone structures or do not have outlets for the fluids to be drained downstream, i.e., they are dangling structures or dead ends (Fig. 4a). Although one may argue that such structures represent structural traps which facilitate fluid-rock interaction and mineralization, they are not favorable for significant ore accumulation because if the fluid did not pass through, new fluids could not come in, and the limited amounts of fluid could only precipitate limited amounts of ore minerals. On the other hand, fast fluid flow is not favorable for mineralization either, as this may not allow sufficient time for ore minerals to precipitate and accumulate in a localized area, especially if fluid-rock interaction is the main mechanism of ore precipitation. This may explain the observation that in most cases, mineralization does not occur within the regional-scale, first-order structures, but rather in the second- and third-order structures. The identification of structures with through-going, but yet not too fast fluid flow, and their relationships with the arterial and backbone structures, remain as the most challenging subject in the hydrodynamic study of mineralization, especially in deep mineral exploration.

Acknowledgements

This study is supported by an NSERC-DG grant (Grant No. RGPIN-2018-06458, to Chi) and a National Natural Science Foundation of China grant (Grant No. 41930428, to Xu). We are grateful to numerous colleagues and former students who have been involved in various research projects related to hydrodynamic studies of mineralization. Thanks are extended to the editorial office of Acta Geologica Sinica and Dr. Fei Hongcai for the invitation to write a review paper on this topic in the occasion of the 100th Anniversary of the Geological Society of China and Acta Geologica Sinica.

Manuscript received Dec. 27, 2021
associate EIC: FEI Hongcai
edited by FANG Xiang

References

Arndt, N.T., Fontbote, L., Hedenquist, J.W., Kesler, S.E., Thompson, J.F.H., and Wood, D., 2017. Future Global Mineral Resources. Geochemical Perspectives, 6: 1–171.

Beaumont, E.A., and Fiedler, F., 1999. Chapter 5: Formation fluid pressure and its application. In: Beaumont, E.A., and Foster, N.H. (eds.), AAPG Treatise of Petroleum Geology/ Handbook of Petroleum Geology: Exploring for Oil and Gas Traps, 5-1–5-64.

Bethke, C.M., 1985. A numerical model of compaction-driven groundwater flow and heat transfer and its application to paleohydrology of intracratonic sedimentary basins. Journal of Geophysical Research, 90: 6817–6828.

Bierlein, F.P., Northover, H.J., Groves, D.I., Goldfarb, R.J., and Marsh, E.E., 2008. Controls on mineralization in the Sierra Foothills gold province, central California, USA: A GIS-based reconnaissance prospectivity analysis. Australian Journal of Earth Sciences, 55: 61–78.

Bjørlykke, K., Mo, A., and Palm, E., 1988. Modelling of thermal convection in sedimentary basins and its relevance to diagenetic reactions. Marine and Petroleum Geology, 5: 338–351.

Blenkinsop, T.G., Oliver, N.H.S., Dirks, P.G.H.M., Nugus, M., Tripp, G., and Sanislav, I., 2020. Structural geology applied to the evaluation of hydrothermal gold deposits. Reviews in Economic Geology, 21: 1–23.

Boiron, M.C., Cathelineau, M., and Richard, A., 2010, Fluid flows and metal deposition near basement/cover unconformity: Lessons and analogies from Pb-Zn-F-Ba systems for the understanding of Proterozoic U deposits. Geofluids, 10: 270–292.

Bons, P.D., Fusswinkel, T., Gomez-Rivas, E., Markl, G., Wagner, T., and Walter, B., 2014. Fluid mixing from below in unconformity-related hydrothermal ore deposits. Geology, 42: 1035–1038.

Burnham, C.W., 1979. Magmas and hydrothermal fluids. In: Barnes, H.L. (ed.), Geochemistry of Hydrothermal Ore Deposits (2nd edition), 71–136.

Burnham, C.W., 1997. Magmas and hydrothermal fluids. In: Barnes, H.L. (ed.), Geochemistry of Hydrothermal Ore Deposits (3rd edition), John Wiley & Sons, New York, 63–123.

Cai, Y., Zhang, J., Li, Z., Guo, Q., Song, J., Fan, H., Liu, W., Qi, F., and Zhang, M., 2015. Outline of uranium resources characteristics and metallogenetic regularity in China. Acta Geologica Sinica, 89: 918–937.

Caine, J.S., Evans, J.P., Foster, C.B., 1996. Fault zone architecture and permeability structure. Geology, 24: 1025–1028.

Card, C.D., 2020. The Patterson Lake corridor of Saskatchewan, Canada: Defining crystalline rocks in a deep-seated structure that hosts a giant, high-grade Proterozoic unconformity uranium system. Geochemistry: Exploration, Environment, Analysis, 21: geochem2020-007.

Cathles, L.M., 1981. Fluid flow and genesis of hydrothermal ore deposits. Economic Geology 75th Anniversary Volume: 424–457.

Cathles, L.M., 1997. Thermal aspects of ore formation. In: Barnes, H.L. (ed.), Geochemistry of Hydrothermal Ore Deposits (Third edition), John Wiley & Sons, New York, 191–227.

Cathles, L.M., 2007. Changes in sub-water table fluid flow at the end of the Proterozoic and its implications for gas pulsars and MVT lead-zinc deposits. Geofluids, 7: 209–226.

Cathles, L.M., and Adams, J.J., 2005. Fluid flow and petroleum and mineral resources in the upper (<20 km) continental crust. In: Hedenquist, J.W., Thompson, J.F.H., Goldfarb, R.J., and Richards, J.P. (eds.), Economic Geology One Hundredth Anniversary Volume, Society of Economic Geologists: 77–110.

Cathles, L.M., and Smith, A.T., 1983. Thermal constraints on the formation of Mississippi Valley-type lead-zinc deposits and their implications for episodic basin dewatering and deposit genesis. Economic Geology, 78: 983–1002.

Chauvet, A., 2019a. Editorial for special issue "Structural Control of Mineral Deposits: Theory and Reality". Minerals, 9: 171.

Chauvet, A., 2019b. Structural control of ore deposits: The role of pre-existing structures on the formation of mineralized vein systems. Minerals, 9: 56.

Chelle-Michou, C., Rottier, B., Caricchi, L., and Simpson, G., 2017. Tempo of magma degassing and the genesis of porphyry copper deposits. Scientific Reports, 7: 40566.

Chen, B.L., Gao, Y., Shen, J.H., Chen, Z.L., Hu, Z.H., Tang, X.S., and Wang, Y., 2021. Study on the ore-bearing fracture system of the Zoujiashan uranium deposit, SE China. Acta Geologica Sinica, 95: 1523–1544 (in Chinese with English abstract).

Chen, Y.C., Pei, R.F., and Wang, D.H., 2006. On metallogenic series–third discussion. Acta Geologica Sinica, 80: 1501–1508 (in Chinese with English abstract).

Chi, G., and Lin, G., 2015. Relationships between hydrodynamics of mineralization and tectonic settings. Geotectonica et Metallogenia, 39: 402–412.

Chi, G., and Lu, H.Z., 1991. Characteristics of fluid phase separation fields in depth- temperature coordinates with emphasis on their significance on localization of hydrothermal deposits. Acta Mineralogica Sinica, 11: 355–362 (in Chinese with English Abstract).

Chi, G., and Savard, M.M., 1998. Basinal fluid flow models related to Zn-Pb mineralization in the southern margin of the Maritimes Basin, eastern Canada. Economic Geology, 93: 896–910.

Chi, G., and Xue, C., 2011. An overview of hydrodynamic studies of mineralization. Geoscience Frontiers, 2: 423–438.

Chi, G., and Xue, C., 2014. Hydrodynamic regime as major control on localization of uranium mineralization in sedimentary basins. Science China Earth Sciences, 57: 2928–2933.

Chi, G., Guha, J., and Lu, H.Z., 1993. Separation mechanism in the formation of proximal and distal tin-polymetallic deposits, Xinlu ore field, southern China–Evidence from fluid inclusion data. Economic Geology, 88: 916–933.

Chi, G., and Dube, B., Williamson, K., Williams-Jones, A.E., 2006a. Formation of the Campbell-Red Lake gold deposit by H_2O-poor, CO_2-dominated fluids. Mineralium Deposita, 40: 726–741.

Chi, G., Qing, H., Xue, C., and Zeng, R., 2006b. Modeling of fluid pressure evolution related to sediment loading and thrust faulting in the Lanping basin–Implications for the formation of the Jinding Zn-Pb deposit, Yunnan, China. Journal of Geochemical Exploration, 89: 57–60.

Chi, G., Xue, C., Lai, J., and Qing, H., 2007. Sand injection and liquefaction structures in the Jinding Zn-Pb deposit, Yunnan, China: indicators of an overpressured fluid system and implications for mineralization. Economic Geology, 102: 739–743.

Chi, G., Liu, Y., and Dube, B., 2009. Relationship between CO_2-dominated fluids, hydrothermal alterations, and gold mineralization in the Red Lake greenstone belt, Canada. Applied Geochemistry, 24: 504–516.

Chi, G., Lavoie, D., Bertrand, R., and Lee, M.K., 2010. Downward hydrocarbon migration predicted from numerical modeling of fluid overpressure in the Paleozoic Anticosti Basin, eastern Canada. Geofluids, 10: 334–350.

Chi, G., Xue, C., Qing, H., Xue, W., Zhang J., and Sun, Y., 2012. Hydrodynamic analysis of clastic injection and hydraulic fracturing structures in the Jinding Zn-Pb deposit, Yunnan, China. Geoscience Frontiers, 3: 73–84.

Chi, G., Bosman, S., and Card, C., 2013. Numerical modeling of fluid pressure regime in the Athabasca basin and implications for fluid flow models related to the unconformity-type uranium mineralization. Journal of Geochemical Exploration, 125: 8–19.

Chi, G., Xue, C., Sun, X., Luo, P., Song, H., Li, S., and Zeng, R., 2017. Formation of a giant Zn-Pb deposit from hot brines injecting into a shallow oil-gas reservoir in sandstones, Jinding, southwestern China. Terra Nova, 29: 312–320.

Chi, G., Li, Z., Chu, H., Bethune, K.M., Quirt, D.H., Ledru, P., Normand, C., Card, C., Bosman, S., Davis, W.J., and Potter, E.G., 2018. A shallow-burial mineralization model for the unconformity-related uranium deposits in the Athabasca Basin. Economic Geology, 113: 1209–1217.

Chi, G., Li, Z., Xu, D., Ledru, P., Chu, H., and Xue, C., 2019a. Coupled control of intra-basinal and deep-seated geologic processes on formation of some super-large uranium and base-metal deposits in sedimentary basins. Proceedings of the 15th Biennial SGA Meeting, August 27–30, Glasgow, Scotland, V1: 36–39.

Chi, G., Chu, H., Petts, D., Potter, E., Jackson, S., and Williams-Jones, A., 2019b. Uranium-rich diagenetic fluids provide the key to unconformity-related uranium mineralization in the Athabasca Basin. Scientific Reports, 9: 5530.

Chi, G., Eldursi, K., Li, Z., Bethune, K., Ledru, P., and Quirt, D., 2019c. Thermal-Hydraulic-Mechanical-Chemical (THMC) Modeling of Fluid Flow and Its Control on Localization of Uranium Deposits in the Northeastern Athabasca Basin, Saskatchewan. Technical Report for the NSERC-CRD and Orano Canada (formerly AREVA) Supported Project, p. 107. DOI: 10.13140/RG.2.2.22018.71366.

Chi, G., Ashton, K., Deng, T., Xu, D., Li, Z., Song, H., Liang, R., and Kennicott, J., 2020. Comparison of granite-related uranium deposits in the Beaverlodge district (Canada) and South China–A common control of mineralization by coupled shallow and deep-seated geologic processes in an extensional setting. Ore Geology Reviews, 117: 103319.

Chi, G., Diamond, L., Lu, H.Z., Lai, J., and Chu, H., 2021. Common problems and pitfalls in fluid inclusion study: A review and discussion. Minerals, 11: 7.

Child, C., Manzocchi, T., Walsh, J.J., Bonson, C.G., Nicol, A., Martin P.J., and Schopfer, M.P.J., 2009. A geometric model of fault zone and fault rock thickness variations. Journal of Structural Geology, 31: 117–127.

Choi, J.H., Edwards, P., Ko, K., and Kim, Y.S., 2016. Definition and classification of fault damage zones: A review and a new methodological approach. Earth-Science Reviews, 152: 70–87.

Cline, J.S., Hofstra, A.H., Muntean, J.L., Tosdal, R.M., and Hickey, K.A., 2005. Carlin-type gold deposits in Nevada: critical geologic characteristics and viable models. Economic Geology 100^{th} Anniversary Volume: 451–484.

Cox, D.P., and Singer, D.A., 1996. USGS Mineral Deposit Models, p. 64–65. http://pubs.usgs.gov/bul/b1693/tlbc.pdf

Cox, S.F., 2005. Coupling between deformation, fluid pressures, and fluid flow in ore-producing hydrothermal systems at depth in the crust. In: Hedenquist, J.W., Thompson, J.F.H., Goldfarb, R.J., and Richards, J.P. (eds.), Economic Geology One Hundredth Anniversary Volume, Society of Economic Geologists: 39–76.

Cox, S.F., 2007. Structural and isotopic constraints on fluid flow regimes and fluid pathways during upper crustal deformation: An example from the Taemas area of the Lachlan orogen, SE Australia. Journal of Geophysical Research, 112: B08208.

Cox, S.F., 2010. The application of failure mode diagrams for exploring the roles of fluid pressure and stress states in controlling styles of fracture-controlled permeability enhancement in faults and shear zones. Geofluids, 10: 217–233.

Cox, S.F., 2016. Injection-driven swarm seismicity and permeability enhancement: Implications for the dynamics of hydrothermal ore systems in high fluid flux, overpressured faulting regimes. Economic Geology, 111: 559–587.

Cox, S.F., 2020. The dynamics of permeability enhancement and fluid flow in overpressured, fracture-controlled hydrothermal systems. Reviews in Economic Geology, 21: 25–82.

Cox, S.F., Knackstedt, M.A., and Braun, J., 2001. Principles of structural control on permeability and fluid flow in hydrothermal systems. Reviews in Economic Geology, 14: 1–24.

Cui, T., Yang, J.W., and Samson, I.M., 2012a. Tectonic deformation and fluid flow: Implications for the formation of unconformity-related uranium deposits. Economic Geology, 107: 147–163.

Cui, T., Yang, J.W., and Samson, I.M., 2012b. Solute transport across basement/cover inter-face by buoyancy-driven thermohaline convection: Implications for the formation of the unconformity-related uranium deposits. American Journal of Science, 312: 994–1027.

Cunningham, C.G., 1978. Pressure gradients and boiling as mechanisms for localizing ore in porphyry systems. U.S.

Geological Survey Journal of Research, 6: 745–754.
Deng, J., Zhai, Y.S., Yang, L.Q., Yang, J.C., Fang, Y., Wan, L., Wang, J.P., and Ding, S.J., 1999. Dynamic simulation of tectonic-fluid-metallogenic system in shear zones. Earth Science Frontiers, 6: 115–127 (in Chinese with English abstract).
Deng, T., Xu, D., Chi, G., Wang, Z., Jiao, Q., Ning, J., Dong, G., and Zou, F., 2017. Geology, geochronology, geochemistry and ore genesis of the Wangu gold deposit in northeastern Hunan Province, Jiangnan Orogen, South China. Ore Geology Reviews, 88: 619–637.
Deng, T., Xu, D., Chi, G., Wang, Z., Chen, G., Zhou, Y., Li, Z., Ye, T., and Yu, D., 2020. Caledonian (Early Paleozoic) veins overprinted by Yanshanian (Late Mesozoic) gold mineralization in the Jiangnan Orogen: A case study on gold deposits in northeastern Hunan, South China. Ore Geology Reviews, 124: 103586.
Dube, B., Williamson, K., McNicoll, V., Malo, M., Skulski, T., Twomey, T., and Sanborn-Barrie, M., 2004. Timing of gold mineralization in the Red Lake gold camp, northwestern Ontario, Canada: New constraints from U-Pb geochronology at the Goldcorp Highgrade Zone, Red Lake mine and at the Madsen mine. Economic Geology, 99: 1611–1641.
Eldursi, K., Chi, G., Bethune, K.M., Li, Z., Ledru, P., and Quirt, D., 2021. New insights from 2- and 3-D numerical modeling on fluid flow mechanisms and geological factors responsible for the formation of the world-class Cigar Lake uranium deposit, eastern Athabasca Basin, Canada. Mineralium Deposita, 56: 1365–1388.
Fayek, M., and Kyser, T.K., 1997. Characterization of multiple fluid-flow events and rare-earth-element mobility associated with formation of unconformity-type uranium deposits in the Athabasca Basin, Saskatchewan. Canadian Mineralogist, 35: 627–658.
Fournier, R.O., 1999. Hydrothermal processes related to movement of fluid from plastic into brittle rocks in the magmatic-epithermal environment. Economic Geology, 94: 1193–1211.
Freeze, R.A., and Cherry, J.A., 1979. Groundwater. Prentice Hall, Englewood Cliffs, New Jersey, 1–604.
Fyfe, W.S., Price, N.J., and Thompson, A.B., 1978. Fluids in the earth's crust. Elsevier, Amsterdam, 383.
Gapais, D., 2018. Tectonics-mineralization relationships within weak continental lithospheres: A new structural framework for Precambrian cratons. BSGF–Earth Sciences Bulletin, 189 (3): 14.
Garven, G., and Raffensperger, J.P., 1997. Hydrogeology and geochemistry of ore genesis in sedimentary basins. In: Barnes, H.L. (ed.), Geochemistry of Hydrothermal Ore Deposits (Third edition), John Wiley & Sons, New York, 125–189.
Garven, G., Ge, S., Person, G.M., and Sverjensky, D.A., 1993. Genesis of stratabound ore deposits in the mid-continent basins of North America. 1. The role of regional groundwater flow. American Journal of Science, 293: 497–568.
Ge, S., and Garven, G., 1992. Hydromechanical modeling of tectonically driven groundwater flow with application to the Arkoma foreland basin. Journal of Geophysical Research, 97: 9119–9144.
Giuliani, G., Li, Y.D., and Sheng, T.F., 1988. Fluid inclusion study of Xihuashan tungsten deposit in the southern Jiangxi province, China. Mineralium Deposita, 23: 24–33.
Goldfarb, R.J., and Groves, D.I., 2015. Orogenic gold: common and evolving fluid and metal sources through time. Lithos, 233: 2–26.
Goldfarb, R.J., and Santosh, M., 2014. The dilemma of the Jiaodong gold deposits: Are they unique? Geoscience Frontiers, 5: 139–153.
Groves, D.I., Goldfarb, R.J., Gebre-Mariam, M., Hagemann, S.G., and Robert, F., 1998. Orogenic gold deposits: A proposed classification in the context of their crustal distribution and relationship to other gold deposit types. Ore Geology Reviews, 13: 7–27.
Guo, F., Li, Z., Deng, T., Qu, M., Zhou, W., Huang, Q., Shang, P., Zhang, C., and Yan, Z., 2020. Key factors controlling volcanic-related uranium mineralization in the Xiangshan Basin, Jiangxi Province, South China: A review. Ore Geology Reviews, 122: 103517.
Hagemann, S.G., and Cassidy, K.F., 2000. Archean orogenic lode gold deposits. Reviews in Economic Geology, 13: 1–68.
Harrison, W.J., and Summa, L.L., 1991. Paleohydrology of the Gulf of Mexico Basin. American Journal of Science, 291: 109–176.
Haszeldine, R.S., Samson, I.M., and Cornford, C., 1984. Quartz diagenesis and convective fluid movement: Beatrice Oilfield, UK North Sea. Clay Minerals, 19: 391–402.
Hedenquist, J.W., and Lowenstern, J.B., 1994. The role of magmatism in the formation of hydrothermal deposits. Nature, 370: 519–527.
Hedenquist, J.W., Arribas, A., and Reynolds, T.J., 1998. Evolution of an intrusion-centered hydrothermal system: Far Southeast-Lepanto porphyry – epithermal Cu-Au deposits, Philippines. Economic Geology, 93: 373–404.
Hobbs, B.E., Zhang, Y., Ord, A., and Zhao, C., 2000. Application of coupled deformation, fluid flow, thermal and chemical modelling to predictive mineral exploration. Journal of Geochemical Exploration 69–70: 505–509.
Hronsky, J.M.A., 2011. Self-organized critical systems and ore formation: The key to spatial targeting? Society of Economic Geology Newsletter, 84: 14–16.
Hu, F.F., Fan, H.R., Jiang, X.H., L, X.C., Yang, K.F., and Mernagh, T., 2013. Fluid inclusions at different depths in the Sanshandao gold deposit, Jiaodong Peninsula, China. Geofluids, 13: 528–541.
Huang, L.J., and Xu, G.F., 2006. Method and technique study for deep resource exploration in mineral resources sections and strips. Acta Geologica Sinica, 80: 1549–1552 (in Chinese with English abstract).
Hubbert, M.K., 1940. The theory of ground-water motion. Journal of Geology, 48: 785–944.
Hubbert, M.K., and Willis, D.G., 1957. Mechanics of hydraulic fracturing. Transactions of the American Institute of Mining, Metallurgical, and Petroleum Engineers, 210: 153–166.
Hubbert, M.K., and Rubey, W.W., 1959. Role of fluid pressure in mechanics of overthrust faulting. Bulletin of the Geological Society of America, 70: 115–166.
Jackson, N.J., Willis-Richards, J., Manning, D.A.C., and Sams, M., 1989. Evolution of the Cornubian ore field, southwest England: Part II. Mineral deposits and ore-forming processes. Economic Geology, 84: 1101–1133.
Jefferson, C.W., Thomas, D.J., Gandhi, S.S., Ramaekers, P., Delaney, G., Brisbin, D., Cutts, C., Portella, P., and Olson, R.A., 2007. Unconformity-associated uranium deposits of the Athabasca Basin, Saskatchewan and Alberta. Bulletin-Geological Survey of Canada, 588: 23–67.
Kennedy, B.M., Kharaka, Y.K., Evans, W.C., Ellwood, A., DePaolo, D.J., Thordsen, J., Ambats, G., and Mariner, R.H., 1997. Mantle fluids in the San Andreas fault system, California. Science, 278: 1278–1281.
Kim, Y.S., Peacock, D.C.P., and Sanderson, D.J., 2004. Fault damage zones. Journal of Structural Geology, 26: 503–517.
Koziy, L., Bull, S., Large, R., and Selley, D., 2009. Salt as a fluid driver, and basement as a metal source, for stratiform sediment-hosted copper deposits. Geology, 37: 1107–1110.
Kyle, J.K., and Li, N., 2002, Jinding: A giant Tertiary sandstone-hosted Zn-Pb deposit, Yunnan, China. Society of Economic Geologists Newsletter, 50: 8–16.
Kyser, K., and Cuney, M., 2015, Chapter 8: Basins and uranium deposits: Mineralogical Association of Canada. Mineralogical Association of Canada, Short Course Series, 46: 225–304.
Landtwing, M.R., Furrer, C., Redmond, P.B., Pethtke, T., Guillons, M., and Heinrich, C.A., 2010. The Bingham Canyon porphyry Cu-Mo-Au deposit, III. Zone copper-gold ore deposition by magmatic vapor expansion. Economic Geology, 106: 91–118.
Leach, D.L., Song, Y.C., and Hou, Z.Q., 2017. The world-class Jinding Zn-Pb deposit: Ore formation in an evaporite dome, Lanping basin, Yunnan, China. Mineralium Deposita, 52: 281–296.
Ledru, P., 2019. The Mineral System concept applied to unconformity-related uranium deposits of the Athabasca Basin

(Canada). In: Proceedings of the 15th SGA Biennial Meeting, Glasgow, Scotland, 1179–1182.

Ledru, P., Benedicto, A., Chi, G., Khairallah, C., Mercadier, J., Poh, J., and Robbins, J., 2022. The unconformity-related uranium mineral system of the Athabasca Basin (Canada). Dans Ressources métalliques 2, Decrée, S. (dir.). ISTE Editions, Londres.

Li, Z., Chi, G., and Bethune, K.M., 2016. The effects of basement faults on fluid convection and implications for the formation of unconformity-related uranium deposits in the Athabasca Basin, Canada. Geofluids, 16: 729–751.

Li, Z., Chi, G., Bethune, K.M., Thomas, D., and Zaluski, G., 2017. Structural controls on fluid flow during compressional reactivation of basement faults: Insights from numerical modeling for the formation of unconformity-related uranium deposits in the Athabasca Basin, Canada. Economic Geology, 112: 451–466.

Li, Z., Chi, G., Bethune, K.M., Eldursi, E., Thomas, D., Quirt, D., and Ledru, P., 2018. Synchronous egress and ingress fluid flow related to compressional reactivation of basement faults: The Phoenix and Gryphon uranium deposits, southeastern Athabasca Basin, Saskatchewan, Canada. Mineralium Deposita, 53: 277–292.

Li, Z., Chi, G., Deng, T., and Xu, D., 2019. Control of reactivated faults on the unconformity-related uranium deposits in the Athabasca Basin, Canada. Geotectonica et Metallogenia, 43: 518–527 (In Chinese with English Abstract).

Li, X.H., Klyukin, Y.I., Steele-MacInnis, M., Fan, H.R., Yang, K.F., and Zoheir, B., 2020. Phase equilibria, thermodynamic properties, and solubility of quartz in saline-aqueous-carbonic fluids: Application to orogenic and intrusion-related gold deposits. Geochimica et Cosmochimica Acta, 283: 201–221.

Li, Q., Song, H., Chi, G., Zhang, G., and Xu, Z., 2021. Genesis of visible gold in pyrite in the Zhaoxian gold deposit, Jiaodong gold province, China: Constraints from EBSD micro -structural and LA-ICP-MS elemental analyses. Ore Geology Reviews, 139: 104591.

Li, Z., Chi, G., Bethune, K.M., Eldursi, K., Quirt, D., Ledru, P., and Thomas, D., 2021. Interplay between thermal convection and compressional fault reactivation in the formation of unconformity-related uranium deposits. Mineralium Deposita, 56: 1389–1404.

Liang, R., Chi, G., Ashton, K., Blamey, N., and Fayek, M., 2017. Fluid compositions and P-T conditions of vein-type uranium mineralization in the Beaverlodge uranium district, northern Saskatchewan, Canada. Ore Geology Reviews, 80: 460–483.

Liu, L., Zhao, Y., and Zhao, C., 2010. Coupled geodynamics in the formation of Cu skarn deposits in the Tongling-Anqing district, China: Computational modeling and implications for exploration. Journal of Geochemical Exploration, 106: 146–155.

Liu, Y., Chi, G., Bethune, K.M., and Dube, B., 2011. Fluid dynamics and fluid-structural relationships in the Red Lake mine trend, Red Lake greenstone belt, Ontario, Canada. Geofluids, 11: 260–279.

Liu, X., Fan, H.R., Evans, N.J., Yang, K.F., Danišík, M., McInnes, B.I.A., Qin, K.Z., and Yu, X.F., 2017. Exhumation history of the Sanshandao Au deposit, Jiaodong: constraints from structural analysis and (U-Th)/He thermochronology. Scientific Reports, 7: 7787.

Lowell, J.D., and Guilbert, J.M., 1970. Lateral and vertical alteration-mineralization zoning in porphyry ore deposits. Economic Geology, 65: 373–408.

Ma, W., Deng, T., Xu, D., Chi, G., Li, Z., Zhou, Y., Dong, G., Wang, Z., Zou, S., Qian, Q., and Guo, S., 2021. Geological and geochemical characteristics of hydrothermal alteration in the Wangu deposit in the central Jiangnan Orogenic Belt and implications for gold mineralization, Ore Geology Reviews, 139: 104479.

McCaffrey, K., Lonergan, L., and Wilkinson, J., 1999. Fractures, fluid flow and mineralization. Geological Society of London Special Publication, 155: 328.

McCuaig, T.C., and Hronsky, J.M.A., 2014. The mineral system concept: the key to exploration targeting. Society of Economic Geologists, Special Publication, 18: 153–175.

McCuaig, T.C., Beresford, S., and Hronsky, J., 2010. Translating the mineral systems approach into an effective exploration targeting system. Ore Geology Reviews, 38: 128–138.

Mercadier, J., Richard, A., and Cathelineau, M., 2012. Boron- and magnesium-rich marine brines at the origin of giant unconformity-related uranium deposits: $\delta^{11}B$ evidence from Mg-tourmalines. Geology, 40: 231–234.

Mu, L., Hu, R.Z., Bi, X.W., Tang, Y.Y., Lan, T.G., Lan, Q., Zhu, J.J., Peng, J.T., and Oyebamiji, A., 2021. New Insights into the origin of the world-class Jinding sediment-hosted Zn-Pb deposit, southwestern China: Evidence from LA-ICP-MS analysis of individual fluid inclusions. Economic Geology, 116: 883–907.

Murphy, H.D., 1979. Convective instabilities in vertical fractures and faults: Journal of Geophysical Research, 84: 6121–6130.

Ni, P., Wang, X., Wang, G., Huang, J., Pan, J., and Wang, T., 2015. An infrared microthermometric study of fluid inclusions in coexisting quartz and wolframite from Late Mesozoic tungsten deposits in the Gannan metallogenic belt, South China. Ore Geology Reviews, 65: 1062–1077.

Norton, D., and Cathles, L.M., 1979. Thermal aspects of ore deposition. In: Barnes, H.L. (ed.), Geochemistry of Hydrothermal Ore Deposits (Second edition), John Wiley & Sons, New York, 611–631.

Oliver, J., 1986. Fluids expelled tectonically from orogenic belts: Their role in hydrocarbon migration and other geologic phenomena. Geology, 14: 99–102.

Oliver, N.H.S., 1996. Review and classification of structural controls on fluid flow during regional metamorphism. Journal of Metamorphic Geology, 14: 477–492.

Oliver, N.H.S., McLellan, J.G., Hobbs, B.E., Cleverley, J.S., Ord, A., and Feltrin, L., 2006. Numerical models of extensional deformation, heat transfer, and fluid flows across basement-cover interfaces during basin-related mineralization: Economic Geology, 101: 1–31.

Pek, A.A., and Malkovsky, V.I., 2016. Linked thermal convection of the basement and basinal fluids in formation of the unconformity-related uranium deposits in the Athabasca Basin, Saskatchewan, Canada. Geofluids, 16: 925–940.

Penczak, R., and Mason, R., 1997. Metamorphosed Archean epithermal Au-As-Sb-Zn-(Hg) vein mineralization at the Campbell Mine, Northwestern Ontario. Economic Geology, 92: 696–719.

Phillips, W.J., 1972. Hydraulic fracturing and mineralization. Journal of Geological Society of London, 128: 337–359.

Poh, J., Yamato, P., Duretz, T., Gapais, D., and Ledru, P., 2020. Precambrian deformation belts in compressive tectonic regimes: A numerical perspective. Tectonophysics, 777: 228350.

Potter, E.G., Tschirhart, V., Powell, J.W., Kelly, C.J., Rabiei, M., Johnstone, D., Craven, J.A., Davis, W.J., Pehrsson, S., and Mount, S.M., 2020, Targeted geoscience initiative 5: Integrated multidisciplinary studies of unconformity-related Uranium deposits from the Patterson Lake Corridor, Northern Saskatchewan. Geological Survey of Canada, Bulletin, 615.

Qin, J.H., Wang, D.H., Chen, Y.C., Zhao, R.Y., Liu, S.B., and Jiang, B., 2020. Research on metallogenic regularity and metallogenic series in ore fields–A case study from the Shuikoushan ore field, Hunan Province. Acta Geologica Sinica, 94: 255–269 (in Chinese with English abstract).

Rabiei, M., Chi, G., Potter, E.G., Tschirhart, V., MacKay, C., Frostad, S., McElroy, R., Ashley, R., and McEwan, B. 2021. Fluid evolution along the Patterson Lake corridor in the southwestern Athabasca Basin: constraints from fluid inclusions and implications for unconformity-related uranium mineralization. Geochemistry: Exploration, Environment, Analysis, 20: geochem2020-029.

Raffensperger, J.P., and Garven, G., 1995. The formation of unconformity-type uranium ore deposits: 1. Coupled groundwater flow and heat transport modeling. American Journal of Science, 295: 581–636.

Ranganathan, V., and Hanor, J.S., 1988. Density-driven groundwater flow near salt domes. Chemical Geology, 74: 173–188.

Rhys, D.A., Lewis, P.D., and Rowland, J.V., 2020. Structural controls on ore localization in epithermal gold-silver deposits: Mineral systems approach. Reviews in Economic Geology, 21: 83–145.

Richard, A., Pettke, T., Cathelineau, M., Boiron, M.C., Mercadier, J., Cuney, M., and Derome, D., 2010. Brine–rock interaction in the Athabasca basement (McArthur River U deposit, Canada): Consequences for fluid chemistry and uranium uptake. Terra Nova, 22: 303–308.

Richard, A., Banks, D.A., Mercadier, J., Boiron, M.C., Cuney, M., and Cathelineau, M., 2011. An evaporated seawater origin for the ore-forming brines in unconformity-related uranium deposits (Athabasca Basin, Canada): Cl/Br and δ^{37}Cl analysis of fluid inclusions. Geochimica et Cosmochimica Acta, 75: 2792–2810.

Richards, J.P., and Tosdal, R.M., 2001. Structural controls on ore genesis. Reviews in Economic Geology, 14: 181.

Ridley, J.R., and Diamond, L.W., 2000. Fluid chemistry of orogenic lode gold deposits and implications for genetic models. Reviews in Economic Geology, 13: 141–162.

Robb, L., 2020. Introduction to ore-forming processes (2nd edition). Wiley-Blackwell, 1–496.

Robert, F., and Kelly, W.C., 1987. Ore-forming fluids in Archean gold-bearing quartz veins at Sigma mine, Abitibi greenstone belt, Quebec, Canada. Economic Geology, 82: 1464–1482.

Robert, F., Poulsen, K.H., Cassidy, K.F., and Hodgson, C.J., 2005. Gold metallogeny of the Superior and Yilgarn cratons. In: Hedenquist, J.W., Thompson, J.F.H., Goldfarb, R.J., and Richards, J.P. (eds.), Economic Geology One Hundredth Anniversary Volume, Society of Economic Geologists, 1001–1033.

Rowland, J.V., and Rhys, D.A., 2020. Applied structural geology of ore-forming hydrothermal systems. Reviews in Economic Geology, 14: 313.

Russell, M.J. 1988. A model for the genesis of sediment-hosted exhalative (SEDEX) ore deposits. In: Zachrisson, E. (ed.), Proc. Seventh IAGOD Symposium. Schweizerbartsche Verlagsbuch handlung: 59–66.

Scibek, J., Gleeson, T., and McKenzie, J.M., 2016. The biases and trends in fault zone hydrogeology conceptual models: global compilation and categorical data analysis. Geofluids, 16: 782–798.

Secor, D.T., 1965, Role of fluid pressure in jointing. American Journal of Science, 263: 633–646.

Sheldon, H.A., and Micklethwaite, S. 2007. Damage and permeability around faults: Implications for mineralization. Geology, 35: 903–906.

Shinohara, H., Kazahaya, K., and Lowenstern, J.B., 1995. Volatile transport in a convecting magma column: Implications for porphyry Mineralization. Geology, 23: 1091–1094.

Sibson, R.H., 1987. Earthquake rupturing as a hydrothermal mineralizing agent. Geology, 15: 701–704.

Sibson, R.H., 1990. Conditions for fault-valve behavior. In: Knipe, R.J., and Rutter, E.H. (eds.), Deformation Mechanisms, Rheology and Tectonics. Geological Society, London, Special Publication, 54: 15–28.

Sibson, R.H., 2001. Seismogenic framework for ore deposition. Reviews in Economic Geology, 14: 25–50.

Sibson, R.H., 2004. Controls on maximum fluid overpressure defining conditions for mesozonal mineralization. Journal of Structural Geology, 26: 1127–1136.

Sibson, R.H., 2019. Arterial faults and their role in mineralizing systems. Geoscience Frontiers, 10: 2093–2100.

Sibson, R.H., and Scott, J., 1998. Stress/fault controls on the containment and release of overpressured fluids: examples from gold-quartz vein systems in Juneau, Alaska, Victoria, Australia, and Otago, New Zealand. Ore Geology Reviews, 13: 293–306.

Sibson, R.H., Moore, J., and Rankin, A.H., 1975. Seismic pumping–A hydrothermal fluid transport mechanism. Journal of the Geological Society, 131: 653–659.

Sibson, R.H., Robert, F., and Poulsen, K.H., 1988. High angle reverse faults, fluid pressure cycling, and mesothermal gold-quartz deposits. Geology, 16: 551–555.

Song, M., Wang, G., Cao, C., and He, C., 2012. Geophysical-geological interpretation and deep-seated gold deposit prospecting in Sanshandao-Jiaojia area, eastern Shandong Province, China. Acta Geologica Sinica, 86: 640–652.

Song, Y.C., Hou, Z.Q., Xue, C.D., and Huang, S.Q., 2020. New mapping of the world-class Jinding Zn-Pb deposit, Lanping basin, southwest China: Genesis of ore host rocks and records of hydrocarbon-rock interaction. Economic Geology, 115: 981–1002.

Song, H., Chi, G., Wang, K., Li, Z., Bethune, K.M., Potter, E.G., and Liu, Y. 2021. The role of graphite in the formation of unconformity-related uranium deposits of the Athabasca Basin, Canada: A case study of Raman spectroscopy of graphite from the world-class Phoenix uranium deposit. American Mineralogists, in press. https://doi.org/10.2138/am-2022-8158.

Steele-MacInnis, M., 2018. Fluid inclusions in the system H_2O-$NaCl$-CO_2: An algorithm to determine composition, density and isochore. Chemical Geology, 498: 31–44.

Steele-MacInnis, M., Lecumberri-Sanchez, P., and Bodnar, R.J., 2012. HOKIEFLINCS_H2ONACL: A Microsoft Excel spreadsheet for interpreting microthermometric data from fluid inclusions based on the PVTX properties of H_2O–NaCl. Computers and Geosciences, 49: 334–337.

Strong, D.F., 1988. A review and model for granite-related mineral deposits. In: Taylor, R.P., and Strong, D.F. (eds.), Recent advances in the geology of granite-related mineral deposits. Canadian Institute of Mining and Metallurgy, 39: 424–445.Su, W., Heinrich, C.A., Pettke, T., Zhang, X., Hu, R., and Xia, B., 2009. Sediment-hosted gold deposits in Guizhou, China: Products of wall-rock sulfidation by deep crustal fluids. Economic Geology, 104: 73–93.

Swarbrick, R.E., Osborne, M.J., and Yardley, G.S., 2002. Comparison of overpressure magnitude resulting from the main generating mechanisms. In: Huffman, A.R., and Bowers, G.L. (eds.), Pressure regimes in sedimentary basins and their prediction. AAPG Memoir, 76: 1–12.

Tanelli, G., 1982. Geological setting, mineralogy and genesis of tungsten mineralization in Dayu district, Jiangxi (People's Republic of China): An outline. Mineralium Deposits, 17: 279–294.

Third Geological Team, 1984, The Jinding Pb-Zn deposit exploration report, Lanping County, Yunnan Province: Yunnan Bureau of Geology and Mineral Resources, 1–449 (in Chinese).

Tosdal, R.M., and Richards, J.P., 2001. Magmatic and structural controls on the development of porphyry Cu ± Mo ± Au deposits. Reviews in Economic Geology, 14: 157–181.

Tosdal, R.M., and Dilles, J.H., 2020. Creation of permeability in the porphyry Cu environment. Reviews in Economic Geology, 21: 173–204.

Turcotte, D.L., and Schubert, G., 2002. Geodynamics (second edition). Cambridge University Press, New York.

Vearncombe, J.R, Blenkinsop, T.G, Reddy, S.M., 2004. Applied structural geology for mineral exploration and mining. Journal of Structural Geology, 26: 989–994.

Wang, J.C., 2010. Elementary issues of metallotectonics. Acta Geologica Sinica, 84: 59–69 (in Chinese with English abstract).

Wang, D.H., Xu, J.X., Zhang, J.J., Li, S.R., Xu, Y.M., Zeng, Z.L., and Chen, Z.H., 2008. Several issues on the deep prospecting in South China. Acta Geologica Sinica, 82: 865–872 (in Chinese with English abstract)

Wang, D.H., Chen, Y.C., Xu, Z.G., Huang, F., Wang, Y., and Pei, R.F., 2020. Metallogenic series group: Discussion on minerogenetic series. Acta Geologica Sinica, 94: 18–35 (in Chinese with English abstract).

Wang, Z.M., Han, R.S., and Zhang, Y., 2020. The control effect of metallotectonic system on lead-zinc metallogenic systems: A case study of the Huize deposit, Yunnan Province. Acta Geologica Sinica, 94: 3008–3023 (in Chinese with English abstract).

Wang, Q., Yang, L., Zhao, H., Groves, D.I., Weng, W., Xue, S., Li, H., Dong, C., Yang, L., Li, D., and Deng, J., 2021. Towards a universal model for orogenic gold systems: a perspective based on Chinese examples with geodynamic, temporal, and deposit-scale structural and geochemical diversity. Earth-Science Reviews, 224: 103861.

Wang, Y., Chi, G., Li, Z., and Bosman, S., 2021. Large-scale thermal convection in sedimentary basins revealed by coupled quartz cementation-dissolution distribution pattern and reactive transport modeling – a case study of the Proterozoic

Athabasca Basin (Canada). Earth and Planetary Science Letters, 574: 117168.
Weatherley, D.K., and Henley, R.W., 2013. Flash vaporization during earthquakes evidenced by gold deposits. Nature Geoscience, 6: 294–298.
Wei, W., Hu, R., Bi, X., Peng, J., Su, W., Song, S., and Shi, S., 2012. Infrared microthermometric and stable isotopic study of fluid inclusions in wolframite at the Xihuashan tungsten deposit, Jiangxi province, China. Mineralium Deposita, 47: 589–605.
Williams, P.J., Barton, M.D., Johnson, D.A., Fontbote, L., De Haller, A., Mark, G., Oliver, N.H.S., and Marschik, R., 2005. Iron oxide copper-gold deposits: Geology, space-time distribution, and possible modes of origin. Economic Geology, 100th Anniversary Volume: 371–405.
Wood, D., and Hedenquist, J., 2019. Mineral exploration: Discovering and defining ore deposits. SEG Discovery, 116: 1–22.
Wyborn, L.A.I., Heinrich, C.A., and Jaques, A.L., 1994. Australian Proterozoic mineral systems: Essential ingredients and mappable criteria: Proceedings of the Australasian Institute of Mining and Metallurgy Annual Conference, Darwin, 5–9 August, 109–115.
Xu, D., Deng, T., Chi, G., Wang, Z., Chen, G., Zou, F., Zhang, J., and Zou S., 2017. Gold mineralization in the Jiangnan Orogenic Belt of South China: Geological, geochemical and geochronological characteristics, ore deposit-type and geodynamic setting. Ore Geology Reviews, 88: 565–618.
Xu, X.W., Niu, L., Hong, T., Ke, Q., Li, H., and Wang, X.H., 2019. Tectonic dynamics of fluids and metallogenesis. Journal of Geomechanics, 25: 1–8 (in Chinese with English abstract).
Xu, D., Chi, G., Nie, F., Fayek, M., and Hu, R., 2021. Diversity of uranium deposits in China–Introduction to the Special Issue. Ore Geology Reviews, 129: 103944.
Xue, C., Chen, Y., Wang, D., Yang, J., and Yang, W., 2003. Geology and isotopic composition of helium, neon, xenon and metallogenic age of the Jinding and Baiyangping ore deposits, northwest Yunnan, China. Science in China, Series D, 46: 789–800.
Xue, C., Chi, G., Chen, Y., Wang, D. and Qing, H., 2006. Two fluid systems in the Lanping basin, Yunnan, China–Their interaction and implications for mineralization. Journal of Geochemical Exploration, 89: 436–439.
Xue, C., Zeng, R., Liu, S., Chi, G., Qing, H., Chen, Y., Yang, J., and Wang, D., 2007. Geologic, fluid inclusion and isotopic characteristics of the Jinding Zn-Pb deposit, western Yunnan, South China: A review. Ore Geology Review, 31: 337–359.
Xue, C., Chi, G., and Xue, W., 2010. Interaction of two fluid systems in the formation of sandstone-hosted uranium deposits in the Ordos Basin: Geochemical evidence and hydrodynamic modeling. Journal of Geochemical Exploration, 106: 226–235.
Xue, C., Chi, G., and Xue, W., 2011. Effects of hydrocarbon generation on fluid flow in the Ordos Basin and relationship with uranium mineralization. Geoscience Frontiers, 2: 439–447.
Xue, C., Chi, G., and Fayek, M., 2015. Micro-textures and in situ sulfur isotopic analysis of spheroidal and zonal sulfides in the giant Jinding Zn-Pb deposit, Yunnan, China: Implications for biogenic processes. Journal of Asian Earth Sciences, 103: 288–304.
Yan, Q., Wang, H., and Chi, G., 2020. Pulsed magmatic fluid releasing in the formation of the Taoxihu Sn polymetallic deposit, Eastern Guangdong, SE China: Evidence from fluid inclusions, cassiterite U–Pb geochronology, and stable isotopes. Ore Geology Reviews, 126: 103724.
Yang, J., Large, R., Bull, S., and Scott, D., 2006. Basin-scale numerical modeling to test the role of buoyancy driven fluid flow and heat transport in the formation of stratiform Zn-Pb-Ag deposits in the northern Mt Isa basin. Economic Geology, 101: 1275–1292.
Zhai, Y.S., 2007. Earth system, metallogenic system to exploration system. Earth Science Frontiers, 14: 172–181 (in Chinese with English abstract).
Zhai, Y.S., Peng, R.M., Deng, J., and Wang, J.P., 2000. Metallogenic system analysis and new-type ore deposits forecast. Earth Science Frontiers, 7: 123–132 (in Chinese with English abstract).
Zhai, Y.S., Deng, J., Peng, R.M., and Wang, J.P., 2010. Metallogenic system theory. Beijing: Geological Publishing House, 1–313 (in Chinese).
Zhang, Y., Robinson, J., and Schaubs, P.M., 2011. Numerical modeling of structural controls on fluid flow and mineralization. Geoscience Frontiers, 2: 449–461.
Zhang, L., Groves, D.I., Yang, L.Q., Sun, S.C., Weinberg, R.F., Wang, J.Y., Wu, S.G., Gao, L., Yuan, L.L., and Li, R.H., 2020. Utilization of pre-existing competent and barren quartz veins as hosts to later orogenic gold ores at Huangjindong gold deposit, Jiangnan Orogen, southern China. Mineralium Deposita, 55: 363–380.
Zhao, C., Mühlhaus, H.B., and Hobbs, B.E., 1997. Finite element analysis of steady-state natural convection problems in fluid-saturated porous media heated from below. International Journal for Numerical and Analytical Methods in Geomechanics, 21: 863–881.
Zhao, C., Hobbs, B.E., and Mühlhaus, H.B., 1998. Analysis of pore-fluid pressure gradient and effective vertical-stress gradient distribution in layered hydrodynamic systems, Geophysical Journal International, 134: 519–526.
Zhao, C., Hobbs, B.E., Mühlhaus, H.B., Ord, A., and Lin, G., 2000. Numerical modeling of double diffusion driven reactive flow transport in deformable fluid-saturated porous media with particular consideration of temperature-dependent chemical reaction rates, Engineering Computations, 17: 367–385.
Zhao, C., Hobbs, B.E., Ord, A., Peng, S., Mühlhaus, H.B., and Liu, L., 2004. Theoretical investigation of convective instability in inclined and fluid-saturated, three-dimensional fault zones. Tectonophysics, 387: 47–64.
Zhong, J., Chen, Y., Chen, J., Qi, J., and Dai, M., 2018. Geology and fluid inclusion geochemistry of the Zijinshan high-sulfidation epithermal Cu-Au deposit, Fujian Province, SE China: Implication for deep exploration targeting. Journal of Geochemical Exploration, 184: 49–65.
Zhou, Y., Xu, D., Dong, G., Chi, G., Deng, T., Cai, J., Ning, J., and Wang, Z., 2021. The role of structural reactivation for gold mineralization in northeastern Hunan Province, South China. Journal of Structural Geology, 145: 104306.
Zhu, Y.S., 2006. Basic theory of mineral resources assessment-theory system between regional metallogeny to mineral exploration. Acta Geologica Sinica, 80: 1518–1527 (in Chinese with English abstract).

About the first and corresponding author

CHI Guoxiang is a professor in the Department of Geology at the University of Regina, Canada. His research interest is mainly in the field of economic geology, hydrodynamics of mineralization, and geofluids, with emphasis on application of fluid inclusion and numerical modeling techniques. His current research focuses on the hydrodynamic control of ore-hosting versus barren structures, especially those related to uranium mineralization. E-mail: Guoxiang.chi@uregina.ca.

About the corresponding author

XU Deru is a professor in the School of Earth Sciences at East China University of Technology. His research focuses on continental margin geodynamics and its relationship to metallogeny, ore-field structures and prediction of mineral resources. In recent years, he has been responsible for and undertaken a series of research projects in association with polymetallic metallogenesis, ore prediction and exploration at various scales in South China, and comprehensive study on the tectonic evolution of the Tethyan tectonic domain and related metallogeny. E-mail: xuderu@ecut.edu.cn.